

DISSERTATION

THE EFFECT OF AGING ON GENE EXPRESSION AND MITOCHONDRIAL DNA
IN THE EQUINE OOCYTE AND FOLLICLE

Submitted by

Lino Fernando Campos-Chillon

Department of Biomedical Sciences

In partial fulfillment of the requirements

For the Degree of Doctor of Philosophy

Colorado State University

Fort Collins, Colorado

Fall 2009

UMI Number: 3400989

All rights reserved

INFORMATION TO ALL USERS

The quality of this reproduction is dependent upon the quality of the copy submitted.

In the unlikely event that the author did not send a complete manuscript and there are missing pages, these will be noted. Also, if material had to be removed, a note will indicate the deletion.



UMI 3400989

Copyright 2010 by ProQuest LLC.

All rights reserved. This edition of the work is protected against unauthorized copying under Title 17, United States Code.



ProQuest LLC
789 East Eisenhower Parkway
P.O. Box 1346
Ann Arbor, MI 48106-1346

COLORADO STATE UNIVERSITY

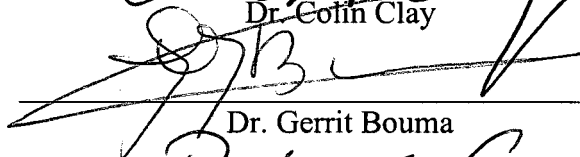
October 15, 2009

WE HEREBY RECOMMEND THAT THE DISSERTATION PREPARED UNDER OUR SUPERVISION BY LINO FERNANDO CAMPOS-CHILLON ENTITLED THE EFFECT OF AGING ON GENE EXPRESSION AND MITOCHONDRIAL DNA IN THE EQUINE OOCYTE AND FOLLICLE BE ACCEPTED AS FULFILLING IN PART REQUIREMENTS FOR THE DEGREE OF DOCTOR OF PHILOSOPHY.

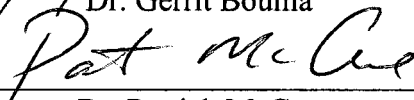
Committee on Graduate Work



Dr. Colin Clay



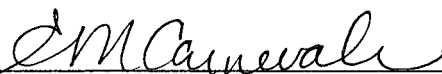
Dr. Gerrit Bouma



Dr. Patrick McCue



Dr. George Seidel



Advisor Dr. Elaine Carnevale



Department Head Dr. Barbara Sanborn

ABSTRACT OF DISSERTATION
THE EFFECT OF AGING ON GENE EXPRESSION AND MITOCHONDRIAL DNA
IN THE EQUINE OOCYTE AND FOLLICLE

The decline in fertility of aged mares is linked to declining oocyte quality. Oocyte viability is dependant on the ability of oocytes to remain in meiotic arrest until the initiation of maturation and adequate cumulus communication. We hypothesize that aging is associated with quantitative and temporal differences in meiotic arrest and resumption in oocytes, decreased oocyte secretion of paracrine factors and lower mitochondrial numbers, ultimately resulting in a dissociation of oocyte and follicular maturation. The objectives of this study were to clone and determine quantitative and temporal differences in mRNA content of the LH receptor (LHR), amphiregulin (AREG) and epiregulin (EREG) in granulosa cells; PDE4 in cumulus cells; and PDE3A, GPR3, GDF9, BMP15, and mitochondrial DNA (mtDNA) in oocytes during in vivo maturation in young (3-12 yr) and old (>20 yr) mares. Oocytes and follicular cells were collected by transvaginal follicular aspiration. Follicle maturation was induced in estrous mares with a follicle > 30 mm by injection of 750 µg of recombinant equine LH. Aspirations were conducted at 0, 6, 9, and 12 h after LH administration. Total RNA was isolated from single denuded oocytes and associated lysed cumulus and granulosa cells. For each gene, mean mRNA copy number for each time point and age group were compared by

ANOVA and Fisher's LSD. Regression coefficients were generated to compare oocyte mitochondrial numbers and correlations between gene expression within age groups. Expression of *LHR* mRNA in granulosa cells was different ($p < 0.05$) between age groups. Young mares displayed a significant drop in *LHR* mRNA between 0 h and 6, 9, and 12 h; while the pattern of expression in old mares was similar ($p > 0.05$) among times and higher ($p < 0.05$) at 6 h than in young mares. Expression of *AREG* mRNA in granulosa cells peaked ($p < 0.05$) at 9 h; however, the magnitude of expression at 6 and 9 h was higher ($p < 0.05$) in old than young mares. Similarly, *EREG* expression peaked ($p < 0.05$) at 9 h in young and old mares but was higher ($p < 0.05$) for old mares. Expression of *PDE4D* peaked ($p < 0.05$) at 6 and 12 h in old and young mares, respectively. The patterns of expression of *GPR3* for oocytes of young and old mares were different and peaked ($p < 0.05$) at 9 and 12 h, respectively. Magnitude of expression of *PDE3A* for oocytes of old mares at 6 and 9 h was higher ($p < 0.05$) than in young mares. Expression of *GDF9* and *BMP15* was different ($p < 0.05$) between ages. Mean expression of both genes in the old group was similar over time; however, in young mare oocytes maximum expression was at 6 h ($p < 0.05$). Correlation coefficients between *GDF9* and *BMP15* for old and young mares were 0.94 and 0.99, respectively. Numbers of copies of oocyte mtDNA did not vary in young mares; however, there was a temporal decrease ($p < 0.05$) of oocyte mitochondrial copy numbers in old mares. The main effect for age for mtDNA was similar for old and young mares.

These results support the idea that asynchronous oocyte maturation in old mares and could explain some aspects of age-associated decline in fertility.

Lino Fernando Campos-Chillón
Biomedical Sciences Department
Colorado State University
Fort Collins, CO 80523-1680
Fall 2009

TABLE OF CONTENTS

CHAPTER	PAGE
I. REVIEW OF THE LITERATURE	1
Introduction	1
Research Animal Models to Study Ovarian Aging	2
Oocyte Maturation	5
Oocyte mRNA Regulation	9
Luteinizing Hormone Receptor	13
Amphiregulin and Epiregulin	14
Phosphodiesterases	16
G-Protein Coupled Receptor 3	19
Cumulus Oocyte Communication	21
GDF9 and BMP15	23
Oocyte Mitochondrial DNA	27
II. VALIDATION OF QRT-PCR AND FOLLICULAR CELL GENOMIC QUANTIFICATION	
Introduction	32
Materials and Methods	33
Gene Cloning	33
Quantitative RT-PCR Validation	34
Granulosa and Cumulus Cell Quantification	36
Results	37
Concluding Remarks	45
III. THE EFFECT OF AGING ON GENE EXPRESSION AND MITOCHONDRIAL DNA IN THE EQUINE OOCYTE AND FOLLICLE	
Introduction	46
Materials and Methods	49
Results	53
Discussion	60
IV. GENERAL CONCLUSION	68
V. REFERENCES CITED	70

CHAPTER I

REVIEW OF LITERATURE

Introduction

The aging process is a complex and multifactorial phenomenon that affects reproductive efficiency. Human fertility trends in western societies indicate women are having fewer children and delaying births to a later age (1). The physiological basis for a decline in fertility in older women involves non-regenerating germ cells, attrition of oocytes, and the subsequent decrease in the number of oocytes from birth ($25\text{-}50 \times 10^4$) to menopause (<1000) (2). In women, the oocyte has been determined to be the primary factor affecting fertility negatively. The transfer of oocytes from younger women reversed the age-associated decline in fertility in older women (3, 4).

A number of theories have been proposed in the last 30 years to explain the age associated decline in fertility in women. One theory is based on changes in endocrine patterns in relation to the decline of the oocyte pool. Such changes include lower circulating levels of E_2 and inhibin β and higher levels of FSH; unfortunately, none of these measurements directly reflects the quality of the oocyte (5). Another theory involves the role of mitochondria and reactive oxygen species (ROS) damage in oocytes

from aged women. This free radical theory proposes that accumulation of ROS over time induces damage and mutations to mitochondrial DNA (6). Furthermore, deprivation of ATP will disrupt mitotic and meiotic spindle formation; most nondisjunction and aneuploidies occur during meiosis, an event of great energy demand (6). Genetic abnormalities are another theory; aneuploidy occurred in 35% of clinical pregnancies among women > 40 years compared to 2% in women < 25 years (1). However, the molecular mechanisms of nondisjunction and aneuploidy need to be further elucidated (1). Another potential theory involves the molecular and cellular components of enhanced apoptosis in aged female germ cells which correlates with the accelerated oocyte depletion of women at the onset of menopause (7). An additional theory emphasizes the meiotic and developmental competence of oocytes in regard to asynchrony of oocyte maturation and ovulation. Delay of ovulation during the menstrual cycle is associated with abnormal ova in women (8).

The origin of age-related decline in fertility continues to be controversial. The majority of hypotheses have attempted to explain the effect in terms of cause and effect, but no single theory is satisfactory. Indeed female fertility is controlled by a series of events occurring at different stages of oocyte development. Most theories agree that the poor oocyte developmental capacity in older women is ultimately related to nuclear and cytoplasmic abnormalities; however, many unanswered questions remain.

Research Animal Models to Study Ovarian Aging

At present, there is no an ideal model to study aging and infertility in women. An ideal animal model to study oocyte developmental competence of aged women would

have similar endocrine and follicular dynamics to women. The rhesus monkey has been used to characterize some of the endocrine and germ cell changes associated with age (9). However, the cost, complexity in management and ethical considerations hamper non-human primate research (10). Rodents are the most widely used model to study ovarian aging. Rodents are recognized for prolific reproduction, uniformity from animal to animal, transgenic models, gene knock-out models and easy management. These attributes, combined with molecular biology tools such as siRNA, microarray and qRT-PCR technology, make rodents a powerful experimental model. However, they are multiparous and their reproductive and molecular events occur rapidly compared to women; in addition, some reproductive endocrine patterns are different than those of women (10) and they have a vastly shorter lifespan. Malhi et al. (11) suggested the cow as a model. Proposed studies involve prediction of ovarian follicle reserve, nuclear and cytoplasmic changes, oocyte and granulosa markers of fertility and elucidation of the role of telomere length. The cow has a short follicular phase and different follicular dynamics than women. Therefore, making direct comparisons with women is difficult.

Ginther et al. (12) characterized the dynamics of follicular waves in mares and women. Some of the remarkable similarities based on reference points and relative values between species were: 1) similar major ovulatory follicular waves, 2) similar major and minor anovulatory waves, 3) numbers of follicles per wave were 5.9 and 3.9 in mares and women, respectively, 3) emergence of dominant follicle to deviation was 4 days for both mares and women, 4) time of dominant follicle deviation to ovulation was 10.1 and 7.4 days in mares and women, respectively, 5) percentage of growth of follicles during the common growth phase were equal and 6) relative diameter of the dominant follicle from

the beginning of deviation to ovulation was similar. In a subsequent study (13), hormonal profiles were analyzed during follicular waves in mares and women, and similar temporal relationships between follicular events and FSH concentrations were observed. These commonalities are only shared by non-human primates; consequently, the mare could be a suitable alternative model.

Reproductive aging in the mare has similar characteristics to humans; fertility declines and reproductive cycles differ with advancing age. Old mares (≥ 20 y) had longer follicular phases and slower growth of the preovulatory follicle (14). In addition, circulating progesterone increased sooner after ovulation in old than young mares, suggesting premature luteinization of the follicle (14). Oocytes collected from the preovulatory follicles of young (6-10 y) and old (20-26 y) pony mares and transferred into oviducts of young, inseminated recipients resulted in pregnancy rates of 92% and 31%, respectively (15). In addition, embryos collected from the oviducts of old mares (≥ 20 years) versus young mares (2-9 y) were delayed in development and had abnormal morphology (16).

Another advantage of the mare for reproductive research is the relative ease of monitoring the reproductive cycle and manipulating large follicles, including follicular injections, oocyte collections, and aspiration of follicular fluid and cells. In addition, the lifespan of the mare is approximately 25 years and exposure to environmental factors is, in part, the same as women. We believe the mare is a feasible model to pursue studies in meiotic and developmental competence of aging oocytes in regard to molecular synchrony of oocyte and follicular maturation due to similarities to women in follicular dynamics and reproductive aging characteristics.

Oocyte Maturation

Oocyte developmental competence has been defined as the ability to resume meiosis, cleave after fertilization, reach the blastocyst stage, establish pregnancy, and ultimately result in normal offspring (17). Molecular synchrony of oocyte maturation can be divided into four events: 1) nuclear maturation, 2) epigenetic maturation 3) cytoplasmic maturation and 4) molecular maturation.

Nuclear maturation includes the reinitiation and completion of meiosis I and arrest in metaphase II, ultimately reducing the number of chromosomes from diploid to haploid. Meiosis is initiated early in fetal development in mammals. Primordial germ cells migrate to the genital ridge and undergo mitotic divisions (18). Then, oogonia enter the first meiotic division and arrest in prophase I until puberty. Oocytes resume meiosis in response to the preovulatory rise in LH. Oocytes at prophase I have an intact nuclear membrane called the germinal vesicle (GV). Resumption of meiosis is characterized by the breakdown of the GV, chromosomal condensation, assembly of the metaphase I spindle and extrusion of the first polar body. A second meiotic spindle is formed, and the oocyte enters meiosis II and arrests at metaphase II until activation by fertilization (19). In women and mares, oocytes are at MII at the time of ovulation.

Epigenetic maturation is defined as stable and heritable chromatin modifications that influence gene expression without changing DNA sequence (20). During oogenesis, germ cells undergo epigenetic modifications that give the genome an imprint that can be maternal or paternal. An important example is methylation of cytosines. Timing of the epigenetic processes of imprinting and maintenance of during oogenesis may alter the

events of oocyte maturation (21). Completion of imprinting is essential for developmental competence of the oocyte and to ultimately establish a normal pregnancy.

Cytoplasmic maturation occurs when the oocyte has completed RNA and protein synthesis, including nucleolus condensation and depletion of ribosomes (17). Other changes involve the redistribution of mitochondria, cortical granules and smooth endoplasmic reticulum. In preparation for oocyte activation by sperm at fertilization, the oocyte develops IP3 sensitivity by increasing the number of receptors in preparation for oocyte activation by sperm at fertilization (21).

Another phase of oocyte maturation has been identified as molecular maturation (17). This form of maturation is the least understood, though some of the components of molecular maturation have been defined. These transcriptional and translational events that occur late in oocyte maturation are likely key factors in producing competent oocytes. Although very limited, both transcription and translation occur after the oocyte reaches its full diameter, and in the early embryo before the maternal-zygotic transition. The mRNA and proteins produced during this time are important components of successful oocyte maturation and subsequent embryo development. Oocytes removed from their follicular environment before completion of all aspects of maturation and placed into an in vitro system had altered expression of mRNA of genes involved in transcription and translation compared to embryos produced in vivo (19). Without proper expression of genes involved in regulating transcription and translation, proteins such as cyclin B1 that are translated from mRNA stores (21) will not be produced when they are needed or at the levels necessary for efficient maturation. Oocyte competence is clearly a

synchronous process that requires coordination of nuclear, epigenetic, molecular and cytoplasmic maturation.

Molecular Events of Oocyte Maturation

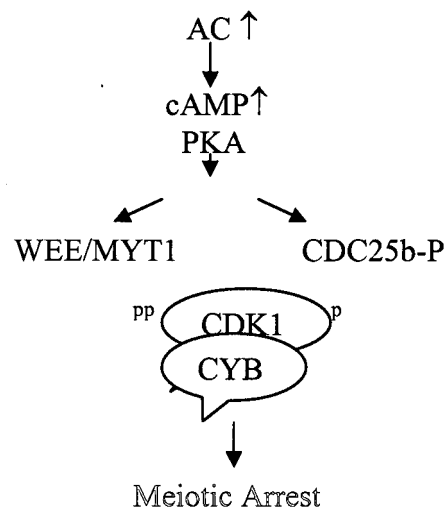
The functional unit in the ovary is the follicle. During the preantral stage, follicular cells divide constantly; when the follicle reaches the antral stage, the cells surrounding the oocyte are called granulosa cells. Granulosa cells become metabolically coupled with each other via gap junctions composed of six subunits of connexins. Granulosa cells are separated by basal laminae from the stromal/theca cells (22). The cells directly surrounding the oocyte differentiate into cumulus cells. Cumulus cells communicate directly with the oocyte via gap junctions, forming a cumulus-oocyte functional unit (22).

In response to the preovulatory LH surge, the oocyte resumes meiosis. However, the molecular pathway of LH signaling to the oocyte needs to be elucidated. Currently, the literature contains contradictory data concerning the role of LH itself. Eppig et al. (23) reported no mRNA for the LH receptor in cumulus cells and oocytes. Yet, in a recent study (24), human oocyte and cumulus cell microarray analyses revealed LH and chorionic gonadotropin receptor overexpression in cumulus cells; however, the presence of the protein was not evaluated. Evidence suggests that the action of LH is on the mural granulosa cells, not the cumulus granulosa cells. Binding of LH to its receptor on mural granulosa cells induces translation of signaling molecules that bind to the granulosa cells, initiating a sequential set of events that eventually lead to oocyte maturation (19).

Although the exact sequence of events occurring in cumulus and granulosa cells is not known, it is clear that signals are transmitted through the gap junctions into the oocyte, which eventually leads to changes in cyclic adenosine monophosphate (cAMP). Meiotic arrest is regulated by cAMP; cAMP is synthesized from ATP by adenyl cyclase and acts as a second messenger in intracellular signal transduction (25). Spontaneous maturation occurs when the oocyte is removed from the follicular environment. In the mouse, the rate of meiotic resumption decreased in experiments using cAMP and/or kinase inhibitors or deletion of phosphodiesterase 3A (25, 26).

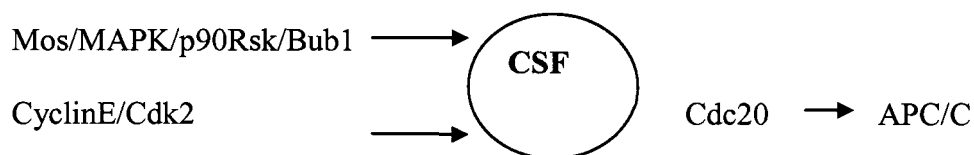
In the oocyte, cAMP regulates the activity of maturation promoter factor (MPF) which is a protein complex of CDK/cyclin B (Fig.1). High levels of cAMP result in the phosphorylation of CDK1 on the Thr 14 and Tyr 15 residues leading to inactivity of MPF (27). A decrease of cAMP leads to the dephosphorylation of CDK1 by protein kinase A (PKA), and MPF becomes active. Protein kinase A regulates the activity of the dual specific phosphatase cdc25 (dephosphorylation of CDK1) and the kinase WEE1/MYT1 (phosphorylation of CDK1) (25).

Figure 1. Cell signaling involved in meiotic arrest



After meiosis I is completed, the oocyte arrests in MII until fertilization. Metaphase II is maintained by cytotstatic factor (CSF) via the mos/MAPK pathway (27) in spite of aligned chromosomes. CSF component Emi2 inhibitor renders anaphase promoting complex (APC/C) inactive. Fertilization leads to the release of intracellular calcium; CSF is destroyed by a calcium activation of Ca^{2+} -dependent calmodulin kinase II by phosphorylation of Emi2 that is further phosphorylated by Plk1 for subsequent destruction by the proteosome (27, 28). The degradation of Emi2 liberates and activates APC/C with subsequent degradation of cyclin B (29). However, a number of pathways have been postulated for the function of CSF in the frog (Fig. 2). Tunquist et al. (28) proposed that CSF is composed of Mos protein in MI, and cyclin E and Cdk2 protein in MII. Mos activity is required for the activation of the MAPK pathway, leading to the Bub1-dependent establishment of CSF arrest. Cyclin E/Cdk2 activity also inhibits APC/C independent of the MAPK pathway. Also, the Cdc20-interacting protein is present in immature oocytes and is necessary for the maintenance of CSF arrest in the oocyte.

Figure 2. Maintenance of CSF



Oocyte mRNA Regulation

Ovarian follicular development is a highly regulated process. Oocytes display post-transcriptional regulatory mechanisms that control mRNA stability and translation. In the nucleus, mRNAs are first transcribed as precursor mRNA (pre-mRNA) and then,

modified by capping, polyadenylation and splicing (30). During oogenesis, the oocyte accumulates mRNA; fully grown oocyte mRNA corresponds to 20-45 % of all mouse genes (31). During oocyte meiotic maturation and the initial stages of embryonic development, the transcriptional machinery is silent. Changes in mRNA abundance in immature and mature oocytes depend on the stability, utilization and degradation of the transcripts involved (32). Maternal mRNA translation is regulated by changes in the 3' poly-A tail length; at the time of meiotic maturation, mRNA polyadenylation is temporally regulated. Polyadenylation involves addition of up to 250 adenosine residues by the poly-A polymerase (33). The cytoplasmic polyadenylation element (CPE) and the hexanucleotide AAUAAA and their interactions with specific CPE binding proteins are necessary to achieve adequate poly-A additions in the cytoplasm (34). A long poly-A allows mRNA to acquire a circular shape prior to translation initiation. Such structure of mRNA is essential for translation efficiency (31).

The half-life of individual mRNA depends on the degradation by exonucleases. Messenger RNA is protected by the methylguanosine cap structure which interacts with the poly-A tail; therefore, shortening of the poly-A at the 3' end leads to mRNA degradation (34). Oocyte mRNAs with short poly-A tails are translational inactive; however, they can be activated by polyadenylation and or inactivated by deadenylation. Cytoplasmic deadenylation mechanisms targeting specific mRNA in mammalian oocytes and the mediators are not know (35). Messenger RNA localization further regulates meiosis; the cytoskeleton is actively involved in transport of mRNA to the site of translation and degradation in the cytoplasm (34). Localization of RNA is involved with spatial restriction in the production of the proteins in the oocyte (35). Maternal mRNA

masking or nonspecific interaction of Y-box proteins involves mRNAs associated with maternal ribonucleoproteins, which prevent binding of mRNA to polyribosomes, and consequently, represses translation (36).

The embryonic genome is activated at later cell cycles. The event is known as the maternal-zygotic transition. This event occurs in the mouse and the cow at the 2-cell and 8-cell stages respectively (36). Mechanisms involved in the maternal-zygotic transition involve degradation of maternal RNA (chromatin mediated repression, deficiency in transcription, and transcription repression or abortion by rapid cell cycles) and increase expression of embryonic genes (37). After fertilization, a rise in calcium oscillations mobilizes maternal mRNAs for translation. The proposed mechanism may involve calcium activation of certain kinases/phosphatases which post-translationally modify RNA binding proteins, releasing the maternal mRNA from repression (32). Micro RNAs have also been involved in maternal-zygotic transition by repressing translation and accelerating mRNA decay (38). The mechanism of action seems to be binding of the short RNAs to the 3' UTR of target mRNA (38).

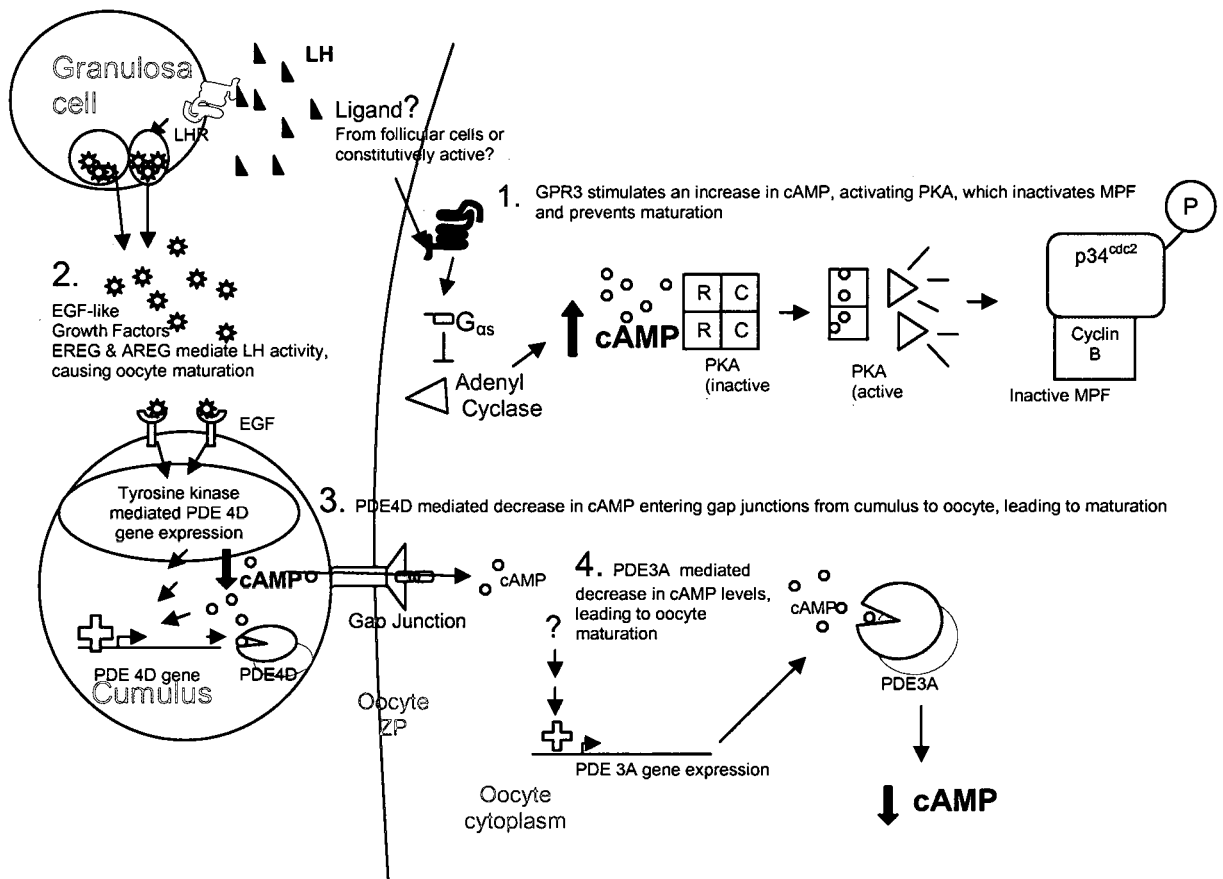
Oocyte mRNA storage and regulation during oocyte maturation and early embryo development are fundamental for embryonic development potential. Gene expression and subsequent translation in oocytes have mRNA specific regulation, and should be studied in individual basis.

Candidate Mechanisms Involved in Resumption of Meiosis

The presence of redundant systems makes it difficult to dissect events in oocyte maturation. A possible pathway for the resumption of meiosis is via LH action on

granulosa cells; the signal is then transmitted to the oocyte, either removing an inhibitory maturation arresting element or providing a positive maturation promoting substance. The model (Fig. 3) involves the following proposed pathway: stimulation of LH on granulosa cells via the LH receptor (LHR), causes release of amphiregulin (AREG), epiregulin (EREG) and betacellulin. Amphiregulin and EREG bind receptors in cumulus cells and mediate phosphodiesterase (PDE) gene expression. Reduction of cAMP in the oocyte may occur because of reduced influx of cAMP via gap junctions from cumulus cells. Indirectly LH activates oocyte-specific PDE3A, resulting in hydrolysis of cAMP. Stimulation of LH may affect indirectly the activity of the ligand that activates the orphan G protein coupled receptor 3 (GPR3) which maintains high levels of cAMP.

Figure 3. Resumption of meiosis model



Luteinizing Hormone Receptor (LHR)

The LHR is a single polypeptide chain classified as a member of the rhodopsin/ β_2 adrenergic receptor subfamily of G protein-coupled receptors (39). The structure includes an extracellular domain (340 amino acid residues), seven transmembrane intracellular and extracellular loops, and a short intracellular C terminus (39). Upon ligand binding, Gs protein is coupled and activates adenylyl cyclase to elevate intracellular cAMP; subsequently, several signaling pathways are activated including protein kinase A, cAMP activated guanine nucleotide exchange factors, and phospholipase C (40). The LHR undergoes broad post-translational modifications; for example, N-linked glycosylation plays a role in the maturation of the receptor, while palmitoylation is involved in receptor endocytosis and post-endocytic trafficking (41). Expression of the LHR not only has been documented in granulosa, luteal and leydig cells, but also, in the oviduct, myometrium, endometrium, vascular smooth muscle of the broad ligament, breast, and ovarian and prostate cancer to name a few (42).

Numbers of receptors in the follicle increase with follicle size and appear at later stages of follicular development, with evidence of a permissive FSH and estradiol action (43). Numbers of LHRs have been associated with follicular deviation; granulosa cells of the dominant follicle had a differential acquisition of *LHR* mRNA just before diameter deviation (44). In the horse, LHR protein content in granulosa cells was greater when follicles were 15–19 mm than in smaller follicles. Similarly, in cattle LHRs were found in granulosa cells from follicles >8mm with no changes in FSH receptors (45).

The preovulatory LH surge or exogenous stimulation with hCG or recombinant LH causes a transient and rapid decline in LHR expression and uncoupling of the LHR

from the G proteins followed by an increase of LHR population as the CL develops (43). Desensitization (transient loss of responsiveness) to LH is due to Gs uncoupling with subsequent decrease of cAMP production, rapid endocytosis of the LHR complex and decrease transcription or degradation of mRNA (39). Recently, down regulation of the LHR was proposed to be caused by a mRNA degradation mechanism (46). In a series of experiments with rat and human granulosa cells, a mRNA binding protein was identified and purified (mevalonate kinase); the protein recognized the open reading frame of the *Lhr* mRNA regulating its stability (46, 47).

At the level of the follicle, LHRs are confined to mural granulosa cells and external theca cells in spite of the profound effects of LH on cumulus cells and the oocyte. Cumulus cells and oocytes failed to respond when exposed to LH in vitro (48, 49). It appears that mural granulosa cells function in an autocrine and paracrine manner after LH stimulation to activate a signaling network of EGF-related ligands (48). Ligand binding of G-protein coupled receptors and subsequent signaling via cAMP has been described to initiate metalloprotease-dependent shedding of EGF-like growth factors and receptors (50). However, the molecular pathway of LH's effect on the oocyte remains unknown.

Amphiregulin and Epiregulin

Epidermal growth factors (EGF) have extensive and important roles in the regulation of cell growth, proliferation, and differentiation. Amphiregulin and EREG are EGF-related proteins that act as mitogens or inhibitors depending on the cell type. Amphiregulin and EREG share a motif of six conserved cysteine residues and an EGF-

like domain (51). They are produced as transmembrane precursors and are cleaved at the cell surface by metalloprotease or disintegrin and metalloprotease families (52). The EGF receptors (EGFR) belong to the tyrosine kinase family. Upon binding, the receptor dimerizes and activates downstream pathways (ERK 1/2). The p38MAPK and ERK1/2 pathways have synergistic and sequential actions in cumulus cells (53). In addition, phosphorylation of the EGFR was indispensable for LH-stimulated oocyte maturation indicating transactivation of the EGF network by LH in preovulatory follicles and amplification of the LH signal (52).

In the mouse, an ovulatory dose of hCG caused expression of *Areg* and *Ereg* mRNAs within 1-3 h after injection (48). In the same study, in situ hybridization revealed expression of these genes restricted to granulosa cells of preovulatory follicles, and no signal was detected in cumulus cells. Amphiregulin and EREG induced cumulus expansion, GV breakdown and nuclear maturation when added to the intact follicle in culture. Furthermore, microarray studies in the mouse indicated maximum levels of *Areg* and *Ereg* at 2 h after administration of hCG in vivo, while in primates, *AREG* and *EREG* increased by 6 and 12 h respectively suggesting a mediatory role in LH action (51). In the mouse and the rat, *Areg* and *Ereg* increased cytoplasmic maturation of in-vitro matured oocytes; however, the effect was not observed with denuded oocytes (54). In the horse, preliminary data indicated maximum mRNA expression of *AREG* and *EREG* at 9 h after exogenous injection of recombinant equine LH (55).

In addition, cumulus cell functions involved neuronal and immune-related up-regulation of genes after LH/EGF stimulation (56). Therefore, cumulus cells may also

provide factors that have the potential to immunoprotect the oocyte and control innate immune responses in the oviduct.

One of the pathways of meiotic resumption appears to be by action of LH on granulosa cells by binding to the LHR followed by rapid production of AREG and EREG, then, transactivation of the EGFR present on cumulus cells and expression of PDE4D and PDE3A in the cumulus cells and oocyte, respectively.

Phosphodiesterases

Regulation and homeostasis of cAMP can occur via extracellular and intracellular mechanisms. Intracellular concentration of cAMP is a balance of synthesis and degradation, and it is regulated by adenylyl cyclase and cyclic nucleotide phosphodiesterases (PDE) (57, 58, 59). There are 11 PDE families, and each isoenzyme serve specific roles, and its expression is fundamental for the specificity of cAMP signaling and compartmentalization (60). The majority of PDE families have more than one gene and generate more than one protein, dependent on different promoters and transcription initiation sites and alternative mRNA splicing; however, the regulation is mostly conserved among species (57). The specificity of the protein is related to the determinants located at the N-terminal portion of the PDE.

Compartmentalization in the cumulus oocyte complexes of PDEs has been established. Cumulus cells and oocytes contain the PDE4D and PDE3A isoforms, respectively (61). The knock-out *Pde4d* mouse model displayed reduced female fertility with 50% decreased litter size; also, the cAMP response to gonadotropins, estrogen production, and ovulation rate decreased (60). Park et al. (62) demonstrated that *Pde4d* is

a gonadotropin regulated gene, and protein accumulation follows activation of transcription, altering intensity and duration of cAMP in follicular cells in vivo and in vitro. The authors concluded that the *Pde4d* gene is epistatic to the progesterone receptor and *Cox-2* genes in upregulation of genes by LH. In the bovid, the type 3 PDE but not the type 4 PDE inhibitors prevented spontaneous maturation of denuded oocytes in vitro, suggesting compartmentalization of PDEs in the follicle (63). In another study, involving bovine intact and denuded oocytes (64), an additive effect of PDE3A but not PDE4D was found on the inhibitory action of theca cell monolayers on oocyte maturation. Also, it was concluded that the factors produced by the theca cell monolayers act upstream from the site of action of PDE3A.

The role of PDE3A in oocyte maturation has been well characterized. In rat oocytes, *Pde3a* was activated prior to resumption of meiosis in both spontaneous and LH-induced maturation in vitro (65). In addition, *Pde3a* activity was only detectable when interactions between oocytes and cumulus cells were maintained. The authors suggested a mechanism in the oocyte involving cAMP degradation, possibly by PKB/Akt phosphorylation of *Pde3a* together with a decrease in permeability of the gap junctions (65, 66, 67). Genetic deletion of *Pde3a* in mice lead to high levels of cAMP in oocytes, persistent activation of PKA and inhibition of MPF/MAPK signaling (68). Further more, *Pde3a*^{-/-} females had oocytes that were not able to resume meiosis. Oocytes remained in prophase I despite normal follicular dynamics and ovulation; in addition, spontaneous maturation did not occur when oocytes were taken out of the follicular environment. In the same study, meiosis was restored by inhibiting protein kinase A (PKA) with adenosine-3',5'-cyclic monophosphorothioate, Rp-isomer (Rp-cAMPS) or by injection of

protein kinase inhibitor peptide (PKI) or mRNA coding for phosphatase CDC25. In swine, *PDE3A* was found also to be the major cAMP degrading PDE in the oocyte; furthermore, it regulated the resumption of meiosis until 3 h prior to GVBD in vitro (69). In the horse, *PDE3A* mRNA was detected 6-9 h in individual oocytes after administration of recombinant equine LH in vivo (55). Microinjection of *Pde3a* into oocytes, arrested with the non-specific inhibitor 3-isobutyl-methylxanthine (IBMX), resulted in GV breakdown (70) demonstrating the specific role of PDEs in resumption of meiosis.

Oocyte maturation studies have shown a beneficial effect of PDE3A inhibitors on cytoplasmic maturation. In the mouse, in vitro exposure of follicle enclosed oocytes to *Pde3a* specific inhibitors for 12 d did not alter follicular cell function, differentiation or oocyte viability (71). Addition of PDE inhibitors delayed GV breakdown and maintained gap junction communications between bovine oocytes and cumulus cells in vitro (72). In the same study, blastocyst rate after in vitro embryo production was significantly increased after 16 h of meiotic arrest with PDE3A and 4D inhibitors. Experimentally in humans, exposure of compact cumulus-oocytes complexes to PDE3A inhibitors during in vitro culture resulted in higher maturation rates and better oocyte morphology; however, fertilization and cleavage rates were the same as controls (73).

Recently, it has been proposed that the effect of LH in cumulus cells and oocytes is mediated by EGF-like factors with subsequent regulation of PDEs (phosphorylation by PKB/AKT); however, further investigation is required.

G-Protein Coupled Receptor 3

The classical model of GPR function involves coupling of the G protein and receptor after ligand stimulation of the receptor. The orphan GPR3 confers constitutive signaling via G α s and generation of cAMP in numerous tissue culture cell lines (74). Structurally, GPR3 is similar to the lysophosphatidic acid receptors and sphingosine-1-phosphate receptors. These groups of receptors are lipid mediators generated from membrane phospholipids and act as intracellular second messengers and extracellular activators of a family of GPCRs(75).

In rodents, *Gpr3* has been found in several tissues; however, in situ hybridization of mouse ovarian sections showed strong *Gpr3* localization in the oocyte. Quantitative RT-PCR resulted in expression of *Gpr3* at 14 times higher levels in the oocyte than in cumulus cells. Most (89%) antral follicles of knock-out mice with deleted *Gpr3* had oocytes that resumed meiosis. In addition, meiotic arrest in *Gpr3*^{-/-} mouse follicle-enclosed oocytes was rescued by injection of RNA encoding *Gpr3* and its Gs subunit (76, 77). In another study (78), *Gpr3* was deleted within the oocyte by microinjecting follicle-enclosed mouse oocytes with siRNA. Oocytes injected with GPR3 siRNA, but not with control siRNA, lost their ability to maintain meiotic arrest. In the rat, microarray analysis and RT-PCR of germinal vesicle oocyte mRNA revealed *Gpr12* and not *Gpr3* to be in control of cAMP levels in oocytes (79).

Regulation of GPRs can be via Gs or Gi, stimulatory or inhibitory subunits, respectively. Localization of the G α sGFP in the plasma membrane versus cytoplasm was smaller in *Gpr3*^{+/+} than in *Gpr3*^{-/-} mouse oocytes as determined with immunofluorescence technology. In addition, injection of *Gpr3* mRNA into *Gpr3*^{-/-} mouse oocytes restored the

cellular localization of G α sGFP, indicating that *Gpr3* activated the Gs signaling pathway (80). In humans, *GPR3* mRNA and Gs protein from immature oocytes was isolated by RT-PCR and western blotting, respectively. Furthermore, injection of immature oocytes with Gs antibodies overcame meiotic inhibition of oocytes cultured with cilostamide (PDE inhibitor) (81). The effect of LH on Gs signaling pathway was studied by monitoring the relative distribution of Gs in mouse oocyte membrane and ooplasm (82); no changes were detected in cellular localization of Gs, suggesting that LH has no effect on the Gs pathway. The effect of LH on the Gi pathway was also evaluated by injection of follicle-enclosed mouse oocytes with pertussis toxin or ethylene diamine tetraacetic acid which inhibits Gi and chelates Ca²⁺ respectively. Both failed to inhibit LH stimulation of oocyte nuclear maturation, suggesting that oocytes lack LH receptors in the membrane that are linked to cAMP via Gi or Ca²⁺ (83). In a genetic approach by mating *Gpr3*^{-/-} with *Pde3a*^{-/-} mice, female infertility was partially rescued (84). It was concluded that *Gpr3* functions upstream of *Pde3a* in regulation of cAMP in oocytes; in addition, cAMP diffusion via gap junctions from follicular cells is not sufficient to maintain meiotic arrest.

Premature ovarian aging has been evaluated in mice deficient in *Gpr3*. Decreased fertility was found in terms of reduced number of zygotes produced by spontaneous ovulation, decreased development to the two-cell and blastocysts stages, and reduced numbers of embryos implanted and litter size (85). In addition, increased levels of FSH and shorter estrous cycles with increased abnormal morphology and fragmentation of oocytes and embryos were observed. These changes mimic some of the characteristics associated with age-related decline of fertility in women (86). However, in an

epidemiological study involving 82 American Caucasian women with premature ovarian failure, no mutations were found in the *GPR3* coding region (87). In the horse, qRT-PCR of individual oocytes from young and old mares revealed a different pattern and magnitude of *GPR3* mRNA expression among ages 0, 6 and 9 h after LH administration (55).

The role of GPR3 in the maintenance of meiotic arrest has been established; however, the link between LH, LHR, AREG, EREG, PDE3A, PDE4D, GPR3 and the levels of cAMP in the oocyte remain to be elucidated.

Cumulus-Oocyte Communication

The intimate association between the oocyte and its surrounding cells is established early in follicular development. Paracrine signals, between the oocyte and follicular cells, are being investigated as regulators of follicular function and fertility. The dogma that follicular and endocrine signals control ovarian activity is being augmented with the concept that the oocyte plays a key role for the coordination of oocyte maturation with follicular development and ovulation. Paracrine factors secreted by oocytes during follicular development are important regulators of granulosa and cumulus cell differentiation (88). In cumulus cells, these factors stimulate cell growth and prevent apoptosis while inhibiting luteinization, LHR expression and inhibin synthesis (88). Fertility can be lost after disruption of oocyte-cumulus communication during early follicular development, follicular growth, preovulation or postovulation (89, 90). The oocyte depends on follicular cells to support its development, regulate meiosis and

modulate gene expression. The cumulus cells undergo expansion while attached to the oocyte; cumulus cells have regulatory effects during ovulation and fertilization (91).

Cumulus oocyte communication is required for normal ovarian folliculogenesis, and oocyte nuclear and cytoplasmic meiotic competence. Gap junctions between the oocyte and surrounding follicular cells are the functional intercellular communication unit (92). Gap junctions are sites of close cell apposition that act as channels, permitting passage of inorganic ions, second messengers and metabolites < 1000 Da. The fundamental unit is the connexon, made of protein subunits termed connexins (93). Connexins (Cx) are composed of four membrane-spanning domains, two extracellular loops, a cytoplasmic loop and cytoplasmic N- and C- terminal (94). In the mouse, *Cx37* are contributed by the oocyte, while *Cx43* are contributed by transzonal projections from cumulus cells docking with *Cx37*, thus forming heterotypic junctions (94). Genetically deficient mice for *Cx37* had impaired oocyte growth (92); while, *Cx43* mutant mice had poorly developed zona pellucidae, vacuolated ooplasm and absence of cortical granules (93).

In the bovid, the onset of germinal vesicle break down occurred when the gap junction communications had dropped to 40%, supporting the idea that gap junction disruption in part induced the nuclear maturation cascade (63). Culture of murine follicle-enclosed oocytes with an inhibitor of *Cx43* caused nuclear maturation after 2 h of exposure (95). Furthermore, LH-induced inhibition of Cx translation was not observed before 3 h after injection, while phosphorylation of *Cx43* occurred within 10 min of LH injection (96). The molecular basis of gap junction disruption after the LH surge is phosphorylation of *Cx43*, mediated by the MAPK pathway (95). A later response

involves inhibition of Cx43 transcription and translation, ultimately eliminating the gap junction channels (96). Further studies are needed to conclude that cAMP produced in somatic cells diffuses into oocytes via gap junctions and could help maintain meiotic arrest.

GDF9 and BMP15

Reproductive aging could change oocyte function, resulting in altered secretion of paracrine factors. These changes could profoundly affect ovarian function and fertility in the old animal or woman. Growth and differentiation factor 9 (GDF9) and bone morphogenetic protein 15 (BMP15) are oocyte specific factors that recently have been studied extensively and possibly interact with the molecular synchrony of oocyte maturation and pass to the cumulus cells via gap junctions.

Growth differentiation factor 9 and BMP15 belong to the transforming growth factor- β (TGF- β) superfamily. Messenger RNA of GDF9 and BMP15 are primarily found in the oocyte of most species (97). Cellular signaling occurs via a receptor complex involving type I and II of membrane bound serine/threonine kinases on granulosa cells (91, 98). The GDF9 signals through an ALK5 type-I receptor, and the downstream signaling is mediated by phosphorylation of Smads 2 and 3 (R-Smads). The receptor for BMP15 is an ALK6 type-Ib receptor, and the intracellular signaling is mediated by phosphorylation of Smads 1, 5 and 8 (R-Smads) (91). In both genes, the R-Smads associate with the co-Smads (Smad 4); this heterodimeric complex translocates from the cytoplasm to the nucleus and regulates transcription of target genes (98)

Mouse knock-out models for *Gdf9* indicated infertility in the female with arrested follicular growth at the primary stage; oocytes had accelerated growth and increased defects (99). Female *Bmp15* knock-out mice were subfertile. Follicular growth was normal but ovulation rates were decreased, and fertilization failure occurred (99). Ewes that had a single copy of a mutation on *GDF9* were fertile and had an increased ovulation rate; in addition, heterozygous for mutations in both *BMP15* and *GDF9* resulted in an additive ovulatory rate (91). Immunization of ewes against BMP15 or GDF9 resulted in impaired fertility; therefore, both are essential for normal follicular development and ovulation rate (97). Furthermore, multiocyte follicles have been reported in mice with single gene mutations in *Gdf9* and *Bmp15* (99).

In mice, knock-out and RNAi experiments suggested *Bmp15* regulation of the preovulatory pattern which involved cumulus expansion and EGF-like molecule expression in cumulus cells (100). Oocyte *Bmp15* was upregulated by gonadotropins and activation of Smad 2 and 3 signaling initiated cumulus expansion by signaling the MAPK pathway that allows FSH/EGF to activate MAPK (98). In another experiment in mice, *Bmp15* promoted glycolysis in cumulus cells and upregulated mRNA encoding glycolytic enzymes (101). Oocytes utilize glucose poorly as energy source, and surrounding cumulus cells provide pyruvate for the oocyte oxidative phosphorylation pathways; therefore, the oocyte directs its somatic cells with metabolites for its own development. Similarly, cholesterol biosynthesis in cumulus cells of mice was regulated by *Bmp15* and *Gdf9* (102). Transcripts encoding enzymes required for cholesterol synthesis were down regulated as well as synthesis of cholesterol from acetate in cumulus cells of mutant mice (*Bmp15*^{-/-} and *Bmp15*^{-/-} *Gdf9*^{+/-}). Since oocytes are inefficient at producing

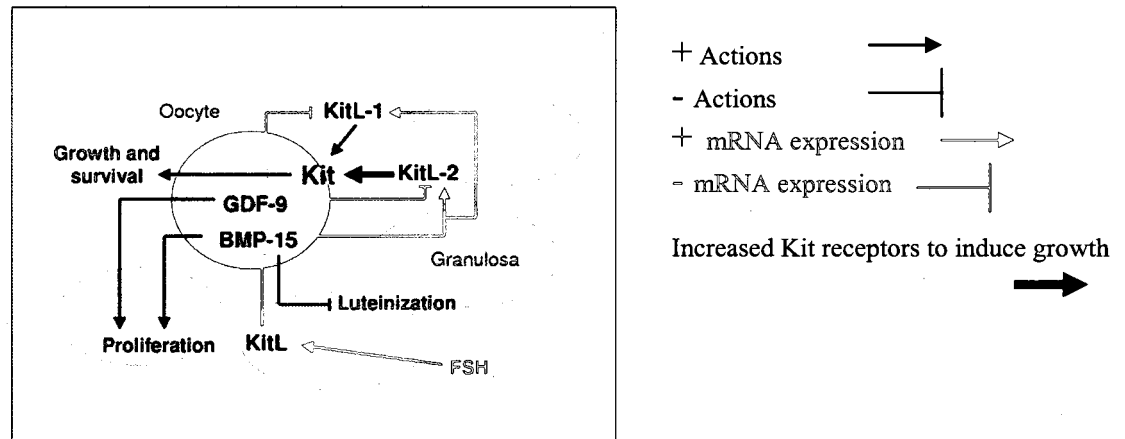
endogenous cholesterol (102), it can be hypothesized that oocytes acquire cholesterol from its micro environment and surrounding cumulus cells. In cattle, GDF9 increased theca cell proliferation and inhibited steroidogenesis in vitro controlling theca interna cell differentiation during follicle growth (103). Also, BMP15 significantly decreased bovine cumulus cell apoptosis in-vitro in a dose dependent manner (104); Bcl-2 (antiapoptotic) was up regulated while Bax expression was down regulated.

Expression of BMP15 and GDF9 mRNA during follicular growth varies among species, *GDF9* was expressed in primordial follicles in cattle, sheep and hamster and in primary follicles in humans and rodents; whereas, *BMP15* was expressed in primary follicles (97). Expression of the mature form of BMP15 protein in mice was detected prior to ovulation after LH treatment and not before, while GDF9 mature protein was detected before the LH surge (105). Messenger RNA of *GDF9* was abundant in bovine oocytes at 55,000 copies per oocyte and was upregulated in competent oocytes. While *BMP15* transcripts were more than 20 fold higher than *GDF9*, expression of *BMP15* was not associated with oocyte competency (106). In the horse, *GDF9* and *BMP15* mRNA were detected at 6 h in individual oocytes after administration of recombinant equine LH in vivo (55). In an epidemiological study involving 38 Caucasian women, mutations of these genes were not linked with premature ovarian failure (107).

Growth differentiation factor 9 and BMP15 pro-proteins are detectable in follicular fluid; however, their direct role in the follicle is not conclusive (106). Close relationships were found between FSH, GDF9, BMP15 and the tyrosine kinase receptor Kit and its ligand, KitL, expressed on oocytes and granulosa cells, respectively (108). The model shows that GDF9 and BMP15 promote proliferation of granulosa cells from

small antral follicles, and BMP15 inhibits FSH-stimulated progesterone production and luteinization. Also, GDF9 suppresses expression of KitL, and BMP15 promotes KitL. Expression of BMP15 is regulated by FSH in a dose-dependent manner via Kit signaling, and Kit signaling promotes both oocyte growth and cell survival (Fig. 4).

Figure 4. FSH, GDF9, BMP15 and KitL communication [Adapted from Thomas et al. (108)]



Both GDF9 and BMP15 have been used successfully during bovine embryo production in vitro (88). Cumulus-oocyte complexes were in vitro matured in serum-free conditions with denuded oocytes for 24 h or for the last 15 h of maturation; blastocyst rates were 51 and 61% per oocyte, respectively, compared to 39% for controls. In the same study, in vitro maturation of oocytes supplemented with recombinant mouse GDF9 and BMP15 resulted in 50 and 58% blastocysts per oocyte, compared to 41% for controls. Similarly, supplementation of murine oocytes with GDF9 increased blastocysts cell numbers in the ICM and most importantly, fetal viability (109). Paracrine communications between the oocyte and its surrounding cumulus and granulosa cells clearly regulate oocyte developmental competence and appear to have profound effects

on developmental programming; however, differences among species exist, and the use of recombinant proteins require caution since the mature form of the protein is the one that has a biological effect.

Oocyte Mitochondrial DNA

Mitochondria play major functions in cell energy, metabolism, homeostasis and death. Mitochondria provide the cell with ATP by oxidative phosphorylation. The respiratory chain involves four complexes located on the inner mitochondrial membrane. The final product is exergonic hydrolysis of ATP to ADP+Pi which provides energy for most energy dependent cell process essential for survival, growth and division (110).

Mitochondria also play a role in several critical cellular pathways leading to synthesis of heme, iron-sulfur proteins, nucleotides, amino acids and calcium homeostasis to name a few (111). In addition, mitochondria produce reactive oxygen species (ROS) and at the same time maintain a ROS-detoxifying enzymatic pathway (reduction of NADPH) (112).

Mitochondrial regulation of apoptosis includes oogenesis and embryonic development; therefore, altered mitochondrial activity has been associated with oocyte and embryo demise. Small numbers of mitochondria (5×10^3) from non apoptotic follicular cells were injected into mouse oocytes and prevented those oocytes from undergoing apoptosis after 24 h of in vitro culture when compared to controls (113).

Mitochondrial DNA

Mitochondria maintain a specific genome, the genome is double-stranded and circular producing ~1% of the 1,500 mitochondrial proteins (114). Mitochondrial DNA (mtDNA) is organized in nucleoids and lacks histones; in addition, the genome is compact without intronic sequences and 5'-3' untranslated regions (112). The control region is known as the D-loop, which includes most regulatory sequences for replication and transcription (114). replication of the mitochondrial genome occurs independently of the cell cycle, and maintenance and repair are done by the same enzymes as in the nucleus; however, mtDNA is more susceptible to damage. Production of reactive oxygen species and lack of histone proteins make mtDNA prone to a high rate of mutations (115).

The mitochondrial genome is maternally transmitted by the oocyte with little or no paternal contribution. Proteasomes in oocytes recognize mitochondria present in the sperm midpiece that was previously ubiquitinated during spermatogenesis. The ubiquitinated epitopes are masked by disulfide bond cross-linking during epididymal passage, and exposed to oocyte induced disulfide bond reduction after fertilization (116).

A genetic bottleneck for the transmission of mtDNA takes place in the primordial germ cells. During oogenesis, mitochondria originate from a small founder population (less than 10 founder mitochondria) and are amplified during oocyte maturation and then reduced. Such restriction and amplification mechanisms seem to reduce the rate of point mutations allowing clonal expansion of a homogeneous set of mtDNA (117). In the mouse, transcripts of replication factors are abundant at the morula and blastocyst stage; however, mtDNA replication occurs at the blastocyst stage, suggesting that the inhibition

of mtDNA replication is controlled at the post-transcriptional level during early embryogenesis (118). It has been suggested that there is one copy of mtDNA per organelle (117). In humans, differentiated oogonia carry ~200 copies; ~6000 copies by prophase-I, and 2×10^5 copies of mtDNA by metaphase II, (118). Mitochondrial numbers among and within oocytes of individuals undergoing assisted reproduction are highly variable with reported 80-fold variation; possibly, the variation is related to the high rate of cytoplasmic growth (119).

Oocyte mitochondrial numbers have been related to developmental competence. In one study using real-time PCR and blocking for male infertility, mtDNA content was lower in cohorts of oocytes from women suffering fertilization failure compared to cohorts with normal fertilization rate after in-vitro fertilization (119). Similarly, mtDNA copies of oocytes from 42 women undergoing ICSI were different between oocytes that failed to fertilize than those that presented with two pronuclei (120).

In the pig, mtDNA copy number, glucose-6-phosphate dehydrogenase content assessed with cresol blue and cytoplasmic transfer demonstrated a significant positive correlation with fertilization outcome (121). In the horse by using real-time PCR, maturation in vitro was associated with mitochondrial degeneration of oocytes from aged mares; in addition, electron microscopy of those oocytes revealed swollen mitochondria with damage cristae (122). In another study, mitochondrial aggregation and metabolic activity were influenced by initial cumulus morphology and stage of in vitro maturation of equine oocytes. Higher metabolic activity was found in oocytes with initial expanded cumulus at the MII stage (123); perhaps higher number of mitochondria is linked with higher metabolic activity and oocyte competence.

Oocyte mitochondrial damage inhibiting GV breakdown, meiotic spindle formation, chromosomal segregation, and polar body extrusion were reversed by germinal vesicle transplantation, and rescued oocytes were able to undergo embryonic development (124). These experiments suggest that mtDNA content could be related to abnormal cytoplasmic maturation that alters fertilization and developmental capacity of oocytes. Furthermore, transfer of ooplasm or mitochondria could improve the fertility of compromised oocytes.

In most mammals, mitochondria of MII oocytes are small, with few cristae distributed throughout the ooplasm and maintain relatively weak energetic activity (110). After fertilization, mitochondria undergo perinuclear localization in response to increased energy demand; inadequate distribution of mitochondria results in poor fertilization and embryonic development (114). It is controversial whether ATP content in oocytes correlates with developmental potential; nonetheless, production of ATP and aerobic use of glucose increase with the first embryonic divisions (111). It has been suggested that constant levels of mtDNA from the MII oocyte to the early embryo reflect a balance between degradation and neosynthesis of the mtDNA (125). Perhaps mitochondrial quality and localization are closely related to developmental competence and ATP content.

Accumulation of mtDNA mutations could be responsible for irreversible cell damage. Lack of histones and limited DNA repair mechanisms may lead to reactive oxygen species damage. Increased mtDNA mutations have been associated with an aging phenotype and an increased rate of apoptosis (126). In a study involving 155 unfertilized

oocytes from young and old women, a significant incidence of a mtDNA mutation (4977 bp deletion) was found in oocytes from women >35 y of age (127).

Mitochondria play a central role in gamete maturation, fertilization and embryo development. Dysfunctions of mitochondria reflect infertility at multiple levels of reproductive processes. The large number of mitochondria in the oocyte may be a genetic rather than a metabolic entity, reassuring the passage of adequate mitochondria to the next generations of primordial germ cells.

CHAPTER II

VALIDATION OF QUANTITATIVE RT-PCR AND QUANTIFICATION OF FOLLICULAR CELLS

Introduction

Methods for gene expression analysis have been widely used to study qualitative and quantitative aspects of gene transcription in somatic and germ cells (oocytes) and developing embryos. Methodologies to quantify mRNA include northern blotting, in-situ hybridization and quantitative real time polymerase chain reaction (qRT-PCR) (128). In northern blotting, the specimen is analyzed by electrophoresis and detection occurs with a hybridization probe. Northern blots provide reliable information on size and integrity of mRNA; however, relative large amounts of tissue are needed. In situ hybridization uses a labeled complementary DNA strand (probe) to localize a specific RNA sequence in a portion or section of tissue, but with low sensitivity. Quantitative RT-PCR offers a big advantage since it detects initial concentrations of mRNA, and its sensitivity permits single-cell mRNA quantification.

Quality control and validation of the qRT-PCR assay are necessary to confirm the sensitivity, specificity and repeatability of the test. The objectives of this series of

experiments were to validate the qRT-PCR assay in single oocytes and follicular cells (<50,000). Initially, the equine sequences for *LHR*, *AREG*, *EREG*, *PDE4D*, *PDE3A*, *GPR3*, *GDF9* and *BMP15* were cloned, followed by *GDF9* and *BMP15* cRNA and plamid DNA q-RT PCR analysis and genomic quantification of follicular cells using the equine CG β gene to asses copy number of CG β per cell.

Materials and Methods

Gene Cloning

Sequences for *LHR*, *AREG*, *EREG*, *PDE4D*, *PDE3A*, *GPR3*, *GDF9* and *BMP15* were examined from data bases of other mammalian species (e.g., cow, mouse, human). Conserved regions among species were determined by alignment of genes using the multiple alignment program (<http://align.genome.jp>). Primers against a conserved region were designed. If the gene has more than one exon, two conserved regions at least 100 base pairs (bp) apart, in one exon and two more of the same in an adjacent exon were selected. Therefore, two polymerase chain reaction (PCR) target sequences were selected 100-150 bp apart, omitting the intron. If the gene only has one exon, primers were design to target two conserved regions within the exon and 100-150 bp apart. Primer design was accomplished using the Oligoperfect program (<http://Invitrogen.com>). The nucleotide-nucleotide BLAST program in the NCBI database, was used to confirm that the primers do not have any homology to any other gene.

Genomic DNA was isolated from equine blood using the Wizard® Genomic DNA Purification Kit (Promega, Madison WI). Polymerase chain reactions were set with 500 ng of genomic DNA using the Expanded High Fidelity PCR System (Roche Applied

Science, Indianapolis IN) and the Robocycler® Gradient 40 (Stratagene, La Jolla CA). Resulting PCR reactions were run on 1% agarose gel with ethidium bromide electrophoresis; if the resulting bands were the correct size, DNA product was purified from the cut bands using QIAEX II Extraction Kit (Qiagen Inc, Valencia CA). The purified DNA was then ligated into pGEM-T Easy Vector (Promega, Madison WI). The ligation reaction and a control ligation were inserted with DH5 α cells (Invitrogen, Carlsbad CA) on ampicillin plates overnight. If a good growth resulted from the incubation, 2-4 colonies were placed in culture medium containing ampicillin and shaken overnight at 37°C. Next, the plasmid was purified using the Qiaprep Spin Miniprep Kit (Qiagen Inc, Valencia CA); the presence of the insert was determined by restricted digest, and the purified product was sent for sequencing (UC Davis Sequencing, Davis CA). Equine specific primers were designed with the same criteria as previously mentioned. In addition, partial cDNA obtained was submitted for sequencing.

Quantitative RT-PCR Validation

The qRT-PCR sensitivity was evaluated by analyzing standard curves, build from cRNA. Plasmid containing equine *GDF9* and *BMP15* was utilized as a template. The plasmids for *GDF9* and *BMP15* were cut and linearized with NCO1 and SAL1 restriction enzymes, respectively. The product was run on 1% agarose gel with ethidium bromide, and DNA was purified from the cut bands of gel using the QIAEX II Extraction Kit. Complementary RNA was obtained using the RiboMax™ Large Scale RNA Production System kit. Concentration and quality (260/280 ratio) of cRNA was obtained using spectrophotometry (NanoDrop, Thermo Scientific, Wilmington DE). Standard dilutions in

duplicates were made to build a standard curve corresponding to 10^{-17} to 10^{-23} moles for each gene. Then, cDNA was obtained for each dilution using the Sensiscript® Reverse Transcription Kit (Qiagen Inc, Valencia CA). Quantitative RT-PCR was performed using the plasmid standard curves (10^{-17} to 10^{-23} moles) previously obtained. Finally, PCR products from the cRNA reactions were run on a 1% agarose gel with ethidium bromide to validate specificity of amplification. Also, amplification curves and cycle threshold values were obtained.

To evaluate the repeatability of the qRT-PCR assay, total RNA was isolated from in vitro matured and denuded bovine oocytes in groups of 1, 50, 75 and 100 using the PicoPure™ RNA Isolation Kit. Each lysate solution was spiked with $\sim 4 \times 10^4$ copies of foreign RNA (DsRed) and served as an exogenous standard to normalize qRT-PCR data. In addition, DNase treatment was performed to improve purity of RNA. Then, cDNA was obtained in replicates for each reaction using the Sensiscript® Reverse Transcription Kit (Qiagen Inc, Valencia CA) with random primers. Quantitative RT-PCR was performed for bovine histone H2a.o variant (129) in duplicates using plasmid standard curves (10^{-16} to 10^{-23} moles) as previously described. Eight-point standard curves (10^{-16} to 10^{-23} moles) were generated for the exogenous control and the genes of interest by serial dilutions of the calculated molarity of the plasmids. The LightCycler® 480 Real-Time PCR System and the LightCycler® 480 SYBR Green I Master detection reagents (Roche Applied Science, Indianapolis IN) were used. Each gene and corresponding standard curves including the spiked gene (DsRed), were run for all samples at the same time in duplicates and with a negative control. The PCR cycle conditions included dissociation for 10 min at 95°C, 45 PCR cycles, dissociation for 5 sec at 95°C, annealing for 5 sec at

58°C, and elongation for 20 sec at 72°C. Data were analyzed by the The LightCycler® 480 Relative Quantification Software (Roche Applied Science, Indianapolis IN), and the correlation coefficients and PCR efficiency for the standard curve were obtained. Melting curves were measured per each sample to validate specificity of amplification. Real-time PCR products were analyzed on a 1% agarose gel with ethidium bromide to confirm specificity.

Granulosa and Cumulus Cell Quantification

Cell quantification after follicular aspirations using a hemocytometer method is time consuming and unreliable. Alternatively, cell quantifications can be accomplished by having several readings (n=7) in the hemocytometer per data point, and then isolating total DNA for each count and plotting total DNA (number of copies of *CGβ*) against a plasmid standard curve (*CGβ*).

Primers for the equine chorionic gonadotropin β (*CGβ*) subunit were designed using the criteria previously discussed. The PCR products were ligated into pGEM-T Easy Vector; then plasmid DNA was purified and sequenced. Total genomic DNA was purified in duplicates using the QIAmp DNA Micro Kit (Qiagen Inc, Valencia CA). Nine data points (1×10^6 to 3 cells) were run in duplicates in the LightCycler® 480 Real-Time PCR System with eight known *CGβ* plasmid standards (10^{-16} to 10^{-23} moles). An equation from the RT-PCR software was generated with a correlation coefficient of >0.98 and a PCR efficiency of $>95\%$.

From a 10 μ l sample from the cell lysate from the RNA isolation step, total genomic DNA was purified using the QIAmp DNA Micro Kit. Then, samples of purified

DNA were run in the LightCycler® 480 Real-Time PCR System with the appropriate plasmid standard curves for *CGβ*. The PCR cycles were the same as for the other genes with an annealing temperature of 60°C. The copy numbers were plotted on the standard curve obtained. Standard curves were generated for granulosa and cumulus cells. Briefly, for a given gene expression data point in moles, it was divided by its corresponding DsRed in moles; then, the result was divided by its corresponding *CGβ* copy number ($\text{POWER}(10, \log \text{moles}) * 6.02 * \text{POWER}(10, 23)$). The obtained value corresponds to corrected value of gene expression over exogenous control in moles per copy number of *CGβ* of cumulus or granulosa cells.

Results

Gene Cloning

The sequenced clones for the horse were successfully obtained and confirmed by sequencing; primers are presented in Table 1. In addition, partial DNA sequences were compared to other species using the BLAST program (Tables 2a and b).

qRT-PCR Validation

GDF9 and *BMP15* cRNA and plasmid DNA amplification curves and cycle thresholds are presented in Figure 4. The coefficients of variation within dilutions were < 8%. The specificity of the PCR products was confirmed with an agarose gel. Band sizes were 150 and 175 bp for *GDF9* and *BMP15* respectively (Fig 5).

Table 1. Primer information for qRT-PCR experiments

Genes	Oligos sequences	Product size (bp)	Annealing Temp (°C)	Intron Spanning
<i>LHR</i>	Forward 5'-tctccccgggtaaaatacc-3' Reverse 5'-cagctgggcatttccctta-3'	271	59	Yes
<i>AREG</i>	Forward 5'-gctgatgggttgaggcac-3' Reverse 5'-ggatattgtggttcgtgtcat-3'	132	58	No
<i>EREG</i>	Forward 5'-aataacgaagtgcagctctga-3' Reverse 5'-gacttgccatgcaaacagt-3'	53	58	No
<i>PDE4D</i>	Forward 5'-gtcccattgtgacagcac-3' Reverse 5'-atcaggatggacgaggtctg-3'	269	59	Yes
<i>PDE3A</i>	Forward 5'-caggcctcactgtgggt-3' Reverse 5'-ggcaggatattccagaca-3'	130	58	Yes
<i>GPR3</i>	Forward 5'-cctgccacctacaacctccat-3' Reverse 5'-caccaggatgcgactagaca-3'	154	60	No
<i>BMP15</i>	Forward 5'-gtgaagcccttgaccaatgt-3' Reverse 5'-aggtgaagttgatggcgta-3'	175	62	Yes
<i>GDF9</i>	Forward 5'-gacttgagtaagtgtccacagca-3' Reverse 5'-cagaggccacctctacaacac-3'	150	62	Yes
DsRed	Forward 5'-gaacgtcatcaccgagttca-3' Reverse 5'-ccttggtcaccttcagcttc-3'	137	58-62	Yes
<i>CGβ</i>	Forward -cagtgtgcacctaccgtgag- Reverse -ggatgtgagaggtgggatg-	221	60	----
mtDNA	Forward -gggccactttacaagaagc- Reverse -agaacagggtctgttagggt-	100	60	----
Bovine H2a.o	Forward 5'-gaggagctgaacaagctgttg-3' Reverse 5'-ttgtggtgctctcagcttcc-3'	104	54	Yes

Table 2a. Equine DNA sequences and percent homology to other species

Gene	Accession #	Homology (%)			
		<i>Homo sapiens</i>	<i>Bos Taurus</i>	<i>Rattus norvegicus</i>	<i>Mus musculus</i>
<i>LHR</i>	GQ183560	99	94	92	89
<i>AREG</i>	DQ238589	87	84	96	92
<i>EREG</i>	DQ238588	93	91	90	79
<i>PDE4D</i>	DQ238590	92	95	92	93
<i>PDE3A</i>	DQ238591	95	88	85	87
<i>GPR3</i>	GQ183561	92	93	87	88
<i>BMP15</i>	GQ183562	89	90	88	84
mtDNA	GQ183565	n/a	n/a	n/a	n/a
<i>GDF9</i>	GQ183563	90	92	82	82
<i>CGβ</i>	GQ183564	78, 82 LHβ	86 LHβ	88 LHβ	82 LHβ

Table 2b. Gene sequences obtained from equine genomic DNA

LHR

TCTCC CCCGGTAAA ATACCTAAGC ATCTGTAACACAGGCATCCG AAAGCTTCCAGATGTTA
CCAAGATCTTCTCCTCTGAAATTAATTTTCATTC TGGAAATTTG CGATAACTTACACATAACCA
CCATACCAGGAAATGCTTTTCAAGGGATGA ATAACGAATCCATAACACTCAAATATATGGA
AATGGACTTGAAGAAAT

AREG

AGTGCTGATGGGTTTGAGGTGACCTCAGGAAGTGAGATCTCCCCTGTGAGTGAAATGCCT
TCTAGTAGCGAACTGCCCTGGGTCTCGACTATGACTATGAAGAAGAGTATGACAACGAA
CCACAAATATCC

EREG

CAATAACGAAGTGCAGCTCTGACATGAATGGCTACTGTTTGCATGGACAATGC

GPR3

CCTGCCACCTACAACCTCCATGATCAACCCCATCATCTATGCCTCCGCAACCAGGACGTGCAG
AAGGTGTTGTGGGCTGTCTGCTGCGGCTGTTCTT

BMP15

GCTGATGCACATGGACATCCTAGAGAGAACCGCACCATTTGGCGCCACCATGGTGAGGCTGGT
GAAGCCCTTGACCAATGTAGCAAGGCCTCTCAGAGGCCCTGGCATATACAGACCCTGGACTT
TCCTCTGAGATCCAACCGGGTAAAATACCAACTAGTCAGAGCCACTGTGGTTTACCGCCATCA
ACTTACCTATCTCACTTCAACCTCTCCTGCTA

GDF9

AGTTGTTGAATGTGTATAACAAGACTGACTTGAGTAAGTGTCCACAGCAGTAACACAATCCA
GGTTAAACAGCAGGTCCACTGACGGAAGGGTTCTGCCACCTGGTCCCCAGGAGCCTGCTTGT
GCTGGGCACAGGGGGTGAAGAGCCGGACAGTGTGTAGAGGTGGCCTCTG

CG β

CAGTGTGCACCTACCGTGAGCTGCGCTTTGCTTCCATCCGGCTCCCCGGCTGCCCGCCTGGTGT
GGACCCCATGGTCTCCTTCCCCGTGGCCCTCAGTTGTCACTGCGGGCCCTGCCAGATCAAGAC
CACTGACTGCGGGGTTTTAGAGACCAGCCCTGGCCTGTGCCCCCAGGCCTCCTTCTCCTCT
AAGGATCCCCCATCCAACCTCTCACATCC

mtDNA

GGGCCCACTTTACAAGAAGCGCCCTCAAACCTAATAGATGACATAATCTAAATCTAACTAATTT
ATAACTTCTACCGCCCTAGAACAGGGCTCGTTAGGGT

The correlation coefficients for the standard curve was 0.996, and PCR efficiency was 1.95. A sensitive assay, as calculated from the plasmid DNA and cRNA of *GDF9* and *BMP15* standard curves was successfully accomplished. Approximately one copy number (10^{-23} moles) was detected at cycles 37 and 39 for *BMP15* and *GDF9*, respectively.

Figure 4. Cycle threshold values of cRNA and plasmid DNA of *GDF9* and *BMP15*

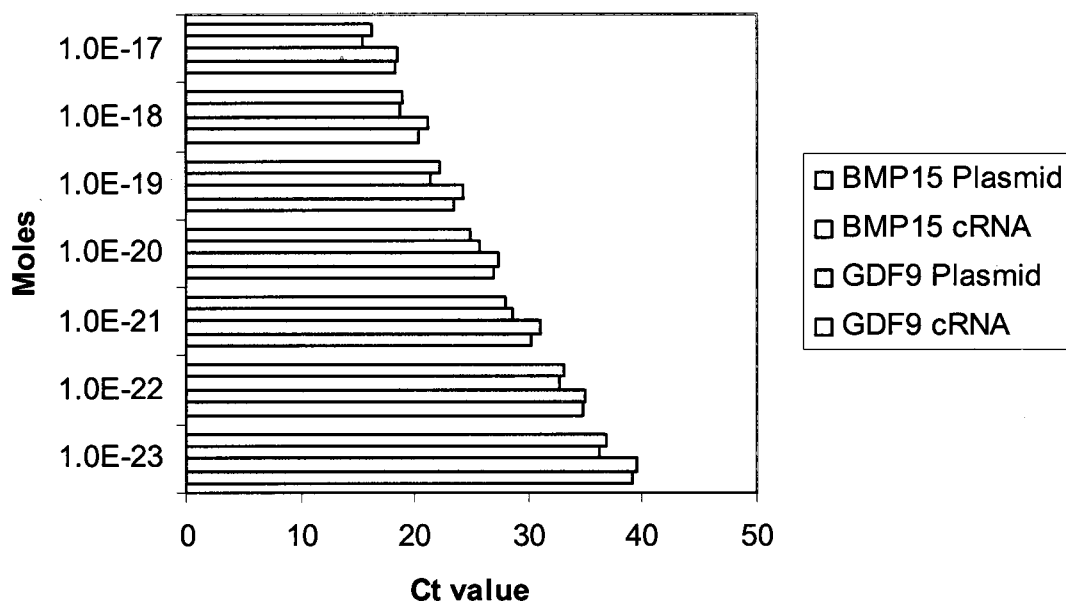
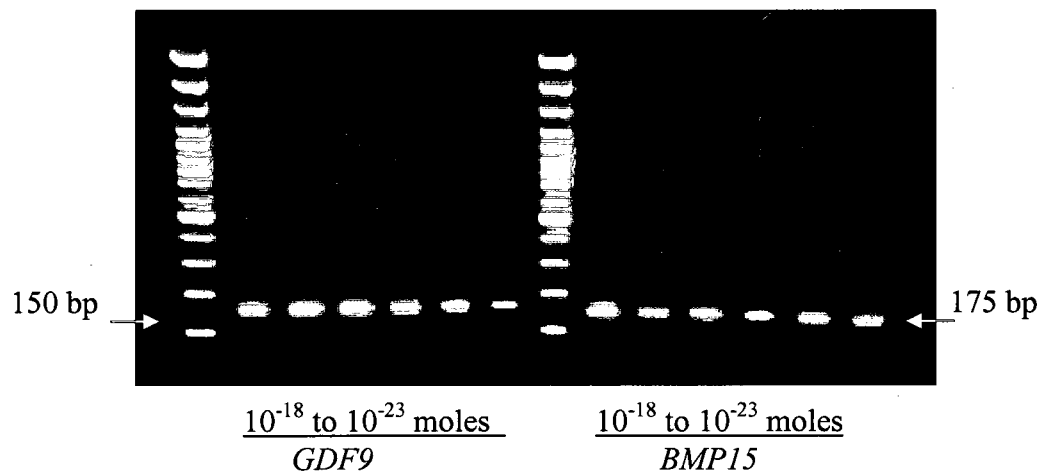


Figure 5. *GDF9* and *BMP15* standard curve qRT-PCR cRNA products



Repeatability of the qRT-PCR assay was confirmed with the Bovine H2a.o gene using matured and denuded bovine oocytes in groups of 1, 50, 75 and 100. Quantifiable message of H2a.o was detected in duplicates, and the fluorescent signal was proportional to the oocyte number (Fig. 6). The correlation coefficient for the standard curve was 0.997 and PCR efficiency was 1.97 (Fig. 7). Melting peaks (Fig. 8) were similar for PCR products of oocytes and standard curves.

Figure 6. Quantitative RT-PCR of H2a.o mRNA isolated from 1, 50, 75 and 100 in vitro matured bovine oocyte

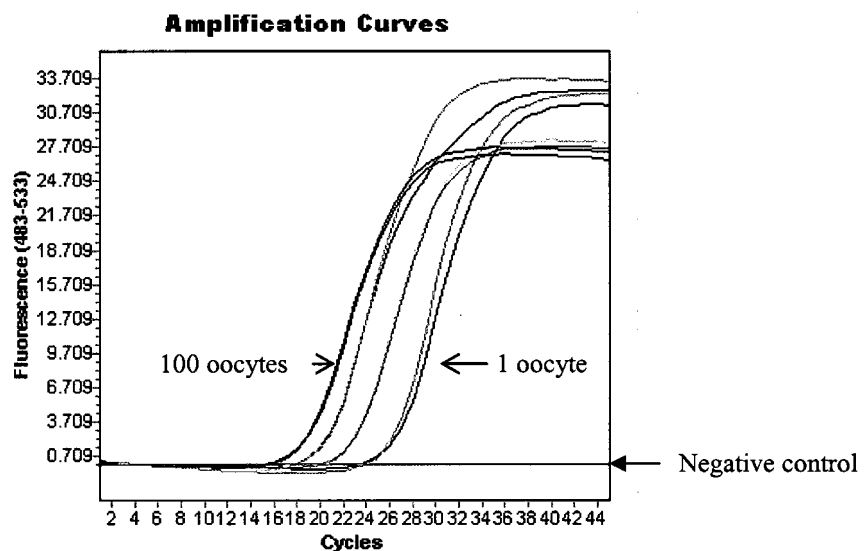
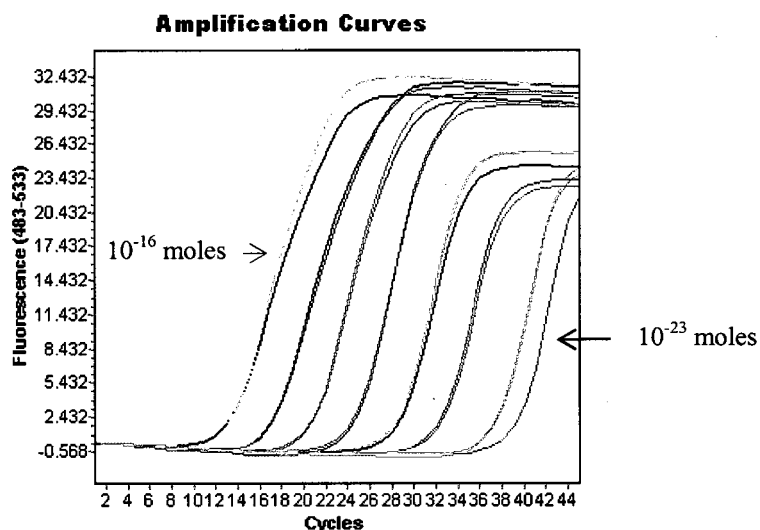


Figure 7. Bovine H2a.o qRT-PCR standard curve amplification



The fluorescent acquisition was 84°C . The sizes of PCR products as analyzed on agarose gel further confirmed the specificity of the reaction for genomic DNA, plasmid DNA (10^{-16} and 10^{-23} moles) and oocytes ($n=1, 50, 75, 100$), (Fig. 9).

Figure 8. Melting peaks for bovine H2a.o qRT-PCR products of oocytes and plasmid standard curves.

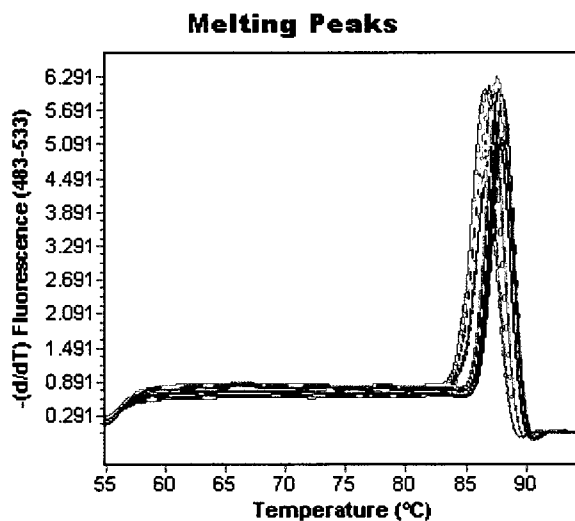
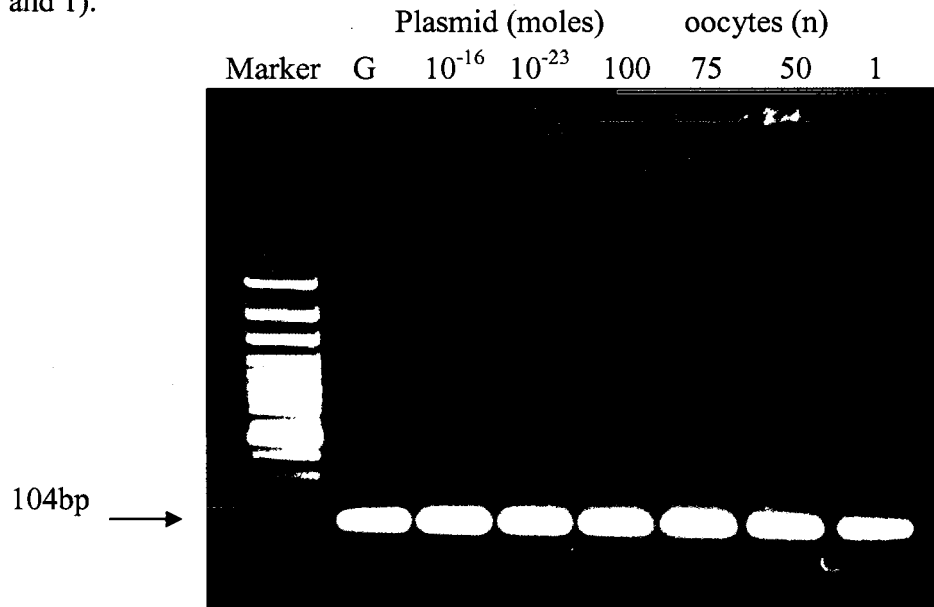


Figure 9. Reaction products of H2a.o qRT-PCR from genomic DNA (G), plamid standard curve (10^{-16} and 10^{-23} moles) and in vitro matured bovine oocytes (n= 100, 75, 50 and 1).



Granulosa and Cumulus Cell Quantification

The efficiencies of the qRT-PCR for genomic *CGβ* of cumulus and granulosa cells were 1.94 and 1.92, respectively. The correlation coefficients for the standard curves made with cell numbers (1.04×10^6 to 3) were 0.998 and 0.997 for cumulus and granulosa cells, respectively. Melting peaks and curves for both types of cells were generated to ascertain specificity of the amplification (Fig. 10). The fluorescence acquisition temperature for *CGβ* was 90°C. Reaction products from the cumulus- and granulosa-cells qRT-PCR when run on a 1% agarose gel with ethidium bromide validated the specificity of the amplification (221 bp) (Fig. 11). Cumulus cell *CGβ* copy number present after removal from oocyte mechanically were 116.52 ± 8.69 SEM.

Figure 10. Melting peaks and curves for *CGβ* of equine granulosa and cumulus cells

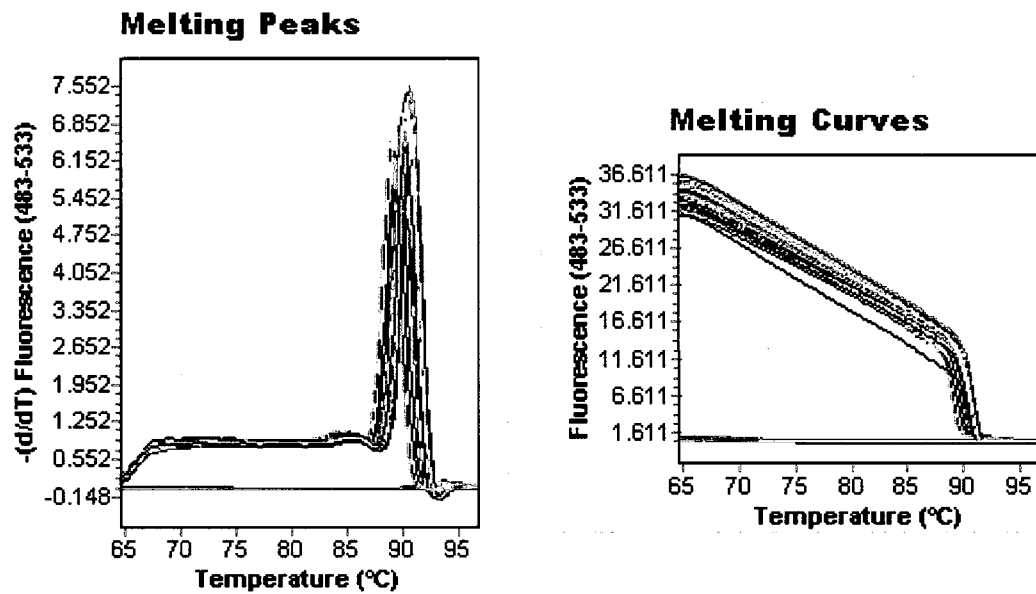
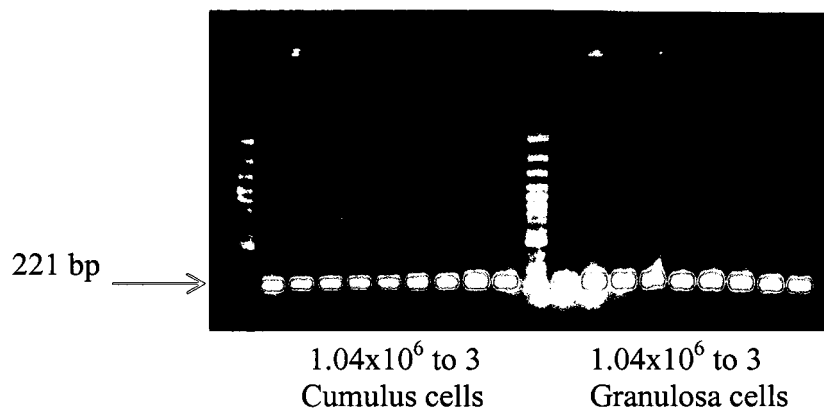


Figure 11. Reaction products of *CGβ* from cumulus and granulosa cells qRT-PCR



Concluding Remarks

The data presented indicate that the LightCycler® 480 Real-Time PCR System conditions in our laboratory were reliable and repeatable. Sensitivity was 10^{-23} moles when using *GDF9* and *BMP15* cRNA and plasmid DNA. Furthermore, detection of bovine H2a.o mRNA of single oocyte mRNA was accomplished with high sensitivity (10^{-23} moles), specificity and repeatability.

Genomic cell correction was also accomplished when using the *CGβ* gene since only two copies per cell are present in the horse prior to the S phase of the cell cycle. Granulosa and cumulus cells (1.04×10^6 to 3) were used to generate standard curves for later cell number (copies of *CGβ*) correction of qRT-PCR of few (<50,000) follicular cells. However, another reliable method warranted would be the use of a house keeping gene such as GADPH or a histone variant for cell number and relative gene expression corrections.

CHAPTER III

THE EFFECT OF AGING ON GENE EXPRESSION AND MITOCHONDRIAL DNA IN THE EQUINE OOCYTE AND FOLLICLE

Introduction

Maternal aging is associated with reduced reproductive efficiency; however, the factors affecting reproduction have not been clearly defined. The physiological basis for a decline in fertility in older women involves nonregenerating germ cells, attrition of oocytes, and a decrease in the number of oocytes from 25 to 50 x 10⁴ at birth to <1000 at menopause (1). In women, oocyte quality is implicated as the primary factor negatively affecting fertility, with this negative effect beginning long before menopause. Transfer of oocytes from younger women reverses the decline in fertility in older women (3,4).

With the exception of the mare, maternal aging has been characterized in few domestic animal species. Reproductive aging in the mare has similar characteristics to humans, with declining fertility and changes in reproductive cycles. Mares ≥ 20 yr are considered old and have longer follicular phases and slower growth of the dominant follicle (14). An earlier increase in circulating progesterone concentrations after ovulation in old than young mares suggests premature luteinization of the follicle (14).

Reduced fertility is observed early after ovulation in the mare, with embryos collected from the oviducts of old mares (≥ 20 yr) versus young mares (2 to 9 yr) being delayed in development and having abnormal morphology (16). As in the woman, maternal aging in the mare appears to affect oocyte quality. When oocytes were collected from the preovulatory follicles of young (6 to 10 yr) and old (20 to 26 yr) pony mares and transferred into oviducts of young, inseminated recipients, pregnancy rates were significantly higher after the transfer of oocytes from young than old mares (92% and 31%, respectively) (15). Therefore, in the woman and mare, oocyte quality appears to be a primary cause of reduced fertility associated with maternal aging; however, distinction between inherent oocyte defects and environmental impacts have yet to be determined.

Oocyte developmental competence is dependent on the ability of oocytes to remain in a state of meiotic arrest until initiation of maturation. The synchrony of oocyte maturation involves nuclear, epigenetic, cytoplasmic and molecular aspects. Several pathways have been proposed for the molecular maturation cascade; however, events between the preovulatory LH surge and reduction of cAMP in the oocyte are still being studied. The orphan G protein-coupled receptor 3 (GPR3) appears to function in maintenance of meiotic arrest. In different genetic mouse models, GPR3 maintained meiotic arrest by elevating intra-oocyte levels of cAMP (76,77). After binding of LH to the LHR, AREG and EREG are released from mural granulosa cells and mediate LH actions in the cumulus-oocyte complex (48,49,51-54). The balance of synthesis and degradation of cAMP is regulated by AC and cyclic nucleotide PDEs, respectively (59,60). Compartmentalization of PDEs in cumulus-oocyte complexes has been

established, with cumulus cells and oocytes containing the PDE4D and PDE3A isoforms, respectively (61).

Cumulus-oocyte communication is required for normal ovarian folliculogenesis and oocyte nuclear and cytoplasmic meiotic competence (92). Two oocyte specific proteins, GDF9 and BMP15, have been linked with follicular development (97). Growth and differentiation factor 9 and BMP15 are detectable in follicular fluid and are involved in events associated with coordination of oocyte maturation and ovulation, including regulation of follicular cell proliferation and viability, increased amino acid transport, decreased numbers of LHRs, decreased luteinization and promotion of glycolysis in cumulus cells (99-102).

Another fundamental factor in oocyte developmental competence is mitochondrial function. Mitochondria play a central role in gamete maturation, fertilization and embryo development (110). Deprivation of ATP could disrupt meiotic arrest and spindle formation. Most nondisjunction and aneuploidies occur during meiosis, an event of great energy demand (110). Genetic abnormalities such as aneuploidy occurred in 35% of pregnancies in women >40 yr compared to 2% in women <25 yr (1). Mitochondrial function has been linked to mitochondrial DNA (mtDNA), with a global decrease in mitochondrial gene expression resulting in compromised oocytes and embryos in women (119).

Reproductive aging could change the expression of key regulatory genes and cumulus-oocyte paracrine factors in the maturation cascade. In addition, mitochondrial dysfunction could result in infertility at multiple levels of reproductive processes. These changes could profoundly affect ovarian function and fertility. Defining the temporal

relationship between LH administration and changes in expression of key transcripts in a monovular species would contribute to our understanding of the oocyte maturation cascade. Aging may result in temporal or quantitative alterations in cellular responses that ultimately affect oocyte quality.

We hypothesized that the quantitative and temporal expression of mRNA for *LHR*, *AREG*, *EREG* in granulosa cells; *PDE4D* in cumulus cells; and *PDE3A*, *GPR3*, *GDF9*, *BMP15* and mtDNA in oocytes are altered in old versus young mares. The primary aims of this study were to characterize gene expression profiles after stimulation with eLH in the mare and to determine if aging affects timing or level of expression of specific genes. Objectives of this experiment were to analyze potential age related differences in the expression profiles of key regulatory genes involved in resumption of meiosis and cumulus-oocyte communications and compare oocyte mitochondrial numbers between young and old mares

Materials and Methods

Gene Cloning

Gene sequences for *LHR*, *AREG*, *EREG*, *PDE4D*, *PDE3A*, *GPR3*, *GDF9* and *BMP15* were searched from other mammalian species (e.g., cow, mouse, human). Conserved regions among species were determined by alignment of genes using CLUSTALW Multiple Sequence Alignment (<http://align.genome.jp>). Primers against conserved regions were designed using the Oligoperfect Program (<http://Invitrogen.com>). Genomic DNA was isolated from equine blood using the Wizard® Genomic DNA Purification Kit (Promega, Madison WI). Polymerase chain reactions were conducted

using 500 ng of genomic DNA and the Expanded High Fidelity PCR System (Roche Applied Science, Indianapolis IN), and performed on the Robocycler® Gradient 40 (Stratagene, La Jolla CA). Following electrophoresis, DNA products were gel purified (QIAEX II Extraction Kit (Qiagen Inc, Valencia CA) and sub-cloned into pGEM-T Easy (Promega, Madison WI). Plasmids were purified using the Qiaprep Spin Miniprep Kit (Qiagen Inc, Valencia CA), and inserts were sequenced (UC Davis Sequencing, Davis CA). After sequencing, equine specific primers for the real-time assays. When possible, primers were designed to span an intron.

Follicular Cells and Oocyte Collection

Oocytes and follicular cells were collected from young mares (3 to 12 yr, n=15) and old mares (≥ 20 yr, n=15). Follicular and oocyte maturation were induced during the follicular phases of mares with a dominant follicle >30 mm in diameter and uterine edema. Granulosa cells, cumulus cells, and oocytes were collected as previously described (130), from dominant follicles of mares at 0, 6, 9 and 12 h after administration of a recombinant equine LH (eLH, 750 μ g, i.v., Aspen Biopharm, Loveland, CO). Briefly a linear ultrasound transducer housed in a plastic casing was placed into the mare's vagina. A 12-gauge, double-lumen needle was placed through the guide in the plastic casing to puncture the vaginal and follicular walls. The follicular contents were aspirated as the follicle was flushed vigorously with 180 ml of medium (EmCare Complete Embryo Flush Solution; ICP, Auckland, New Zealand) supplemented with 10 IU/ml of heparin (Calbiochem; La Jolla, CA) at 37°C. Upon recovery, 5 μ l of medium containing granulosa cells was collected and washed five times in PBS supplemented with 0.02%

polyvinyl alcohol and stored in 20 μ l of Extraction Buffer (PicoPure™ RNA Isolation Kit, Arcturus, Sunnyvale, CA). Cumulus cells were removed mechanically under a stereomicroscope, and 5 μ l of medium containing cumulus cells was processed as described for granulosa cells. The partially denuded oocyte was isolated, washed five times, and placed in 10 μ l of Extraction Buffer. Samples were stored at -80°C until RNA isolation.

Total RNA Extraction

Total RNA isolations from individual oocytes, granulosa cells, and cumulus cells were performed using the PicoPure™ RNA Isolation Kit (Arcturus, Sunnyvale, CA). Samples were thawed at 42°C and processed for RNA isolation. Each lysate solution was spiked with $\sim 4 \times 10^4$ copies of DsRed cRNA (131) which served as an exogenous standard to normalize qRT-PCR data. In addition, 5- μ l from each cell lysate was saved to calculate mitochondrial DNA in oocytes, and to estimate equine chorionic gonadotropin β (CG β) genomic DNA copy number in cumulus and granulosa cells. RNA samples were treated with DNase (Qiagen Inc, Valencia, CA) and stored at -80°C. Complementary DNA (cDNA) was generated from each RNA sample using the Sensiscript® Reversed Transcription Kit (Qiagen Inc, Valencia, CA) with random primers.

Quantitative Real-Time PCR

Eight-point standard curves (10^{-16} to 10^{-23} moles) were generated for DsRed and the genes of interest by serial dilutions of the plasmids based on their calculated molarity. Real-time PCR was performed with the LightCycler® 480 Real-Time PCR System and

the LightCycler® 480 SYBR Green I Master detection reagent (Roche Applied Science, Indianapolis, IN). Each gene, and corresponding standard curves including DsRed, was analyzed in all samples in duplicates, including a –RT negative control. PCR amplification cycle conditions include dissociation for 10 min at 95°C, and 45 cycles at 5 sec at 95°C, annealing for 5 sec at gene specific temperatures (Table 1), and 20 sec at 72°C. PCR products were analyzed on a 1% agarose gel with ethidium bromide to confirm specificity. Data were analyzed by the LightCycler® 480 Basic Software (Roche Applied Science, Indianapolis IN) and normalized to DsRed and number of copies of CG β in cumulus and granulosa cells. Primer specificity was further confirmed using dissociation curve analysis for each primer pair.

Follicular Cells and Oocyte Mitochondrial DNA Quantification

Primers for the CG β subunit (expressed in cumulus and cells) and mtDNA were designed (Table 1). PCR products were ligated into pGEM-T Easy Vector, and plasmid DNAs were purified and sequenced. Genomic DNA was purified from 5- μ l cell lysate (Total RNA Extraction) using the QIAmp DNA Micro Kit (Qiagen Inc, Valencia CA). Samples were run in triplicates on the LightCycler® 480 Real-Time PCR System with eight CG β and mitochondrial plasmid standard points (10^{-16} to 10^{-23} moles). The mitochondria copy number in oocytes was corrected for mitochondria in cumulus and granulosa cells that are attached to oocytes using the average of mitochondrial copies per CG β gene copy.

Statistical Analysis

A factorial experimental design was used with two mare ages (old and young), and four times (0, 6, 9 and 12 h after administration of eLH). Six to ten samples per age and time for oocytes and cumulus cells and 15 samples per age and time for granulosa cells were analyzed. Resulting moles from qRT-PCR were normalized for DsRed, then for *CGβ* copy number. Residual versus predicted value plots were used to evaluate normality of data and homogeneity of variance, respectively. Data were analyzed with SAS (Statistical Analysis System, Cary NC); normalized data were log transformed and evaluated by ANOVA and Fisher LSD. Linear regression coefficients were generated to compare oocyte mitochondrial copy numbers and correlation coefficients among gene expression within age groups.

Results

Gene identity

Sequenced fragments obtained after PCR cloning had >99% homology when compared with the recently published equine genome (www.uky.edu/Ag/Horsemap) (Table 2a and 2b).

Follicular cells

Expression of *LHR* mRNA in granulosa cells varied between young and old mares after administration of eLH. Young mares displayed a significant decline in the *LHR* mRNA between 0 and 6, 9 and 12 h, while the pattern of expression in old mares was not different over time and was higher ($P < 0.05$) at 6 h compared to young mares (Figure 1).

Granulosa cell *LHR* mRNA

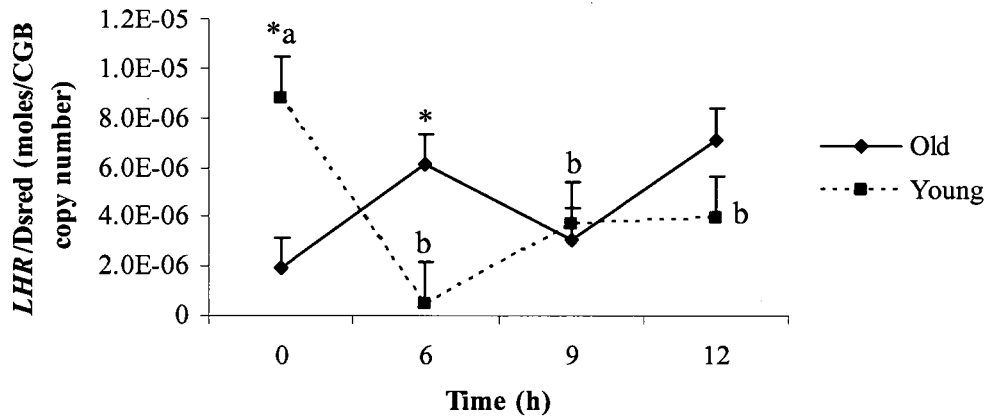
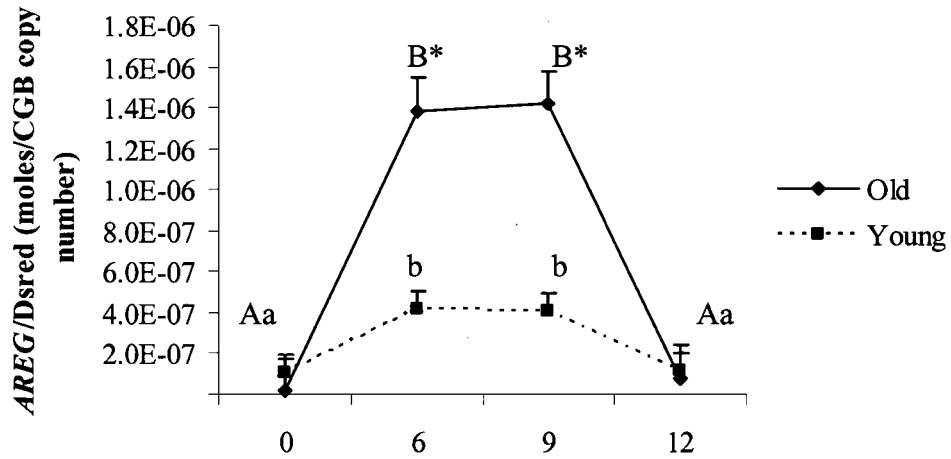


Figure 1. Quantitative expression (means \pm SEM) of *LHR* mRNA in granulosa cells before (0 h) and 6, 9 and 12 h after administration of eLH. ^{ab} Values with different superscript are different ($P < 0.05$) over time for young mares. Values were not different over time for old mares. * $P < 0.05$ young and old mares. Data normalized to DsRed and number of CG β copies.

Expression of mRNA for *AREG* in the granulosa cells of young and old mares was increased ($P < 0.05$) at 6 and 9 h, with higher ($P < 0.05$) expression for old mares than young mares (Fig. 2). Expression of *EREG* in granulosa cells increased ($P < 0.05$) at 9 h in young and old mares but was higher ($P < 0.05$) for old mares (Fig. 2). Correlation coefficients within age between *AREG* and *EREG* for old and young mares were 0.04 and 0.4, respectively.

Expression of *PDE4D* mRNA in cumulus cells was different ($P < 0.05$) between young and old mares at 6, 9 and 12 h, with increased ($P < 0.05$) expression by 6 h in old mares and 12 h in young mares, respectively (Fig. 3). There was an interaction ($P < 0.05$) of age by time in the expression of *PDE4D* from 9 to 12 h (Fig. 3).

Granulosa cell *AREG* mRNA



Granulosa cell *EREG* mRNA

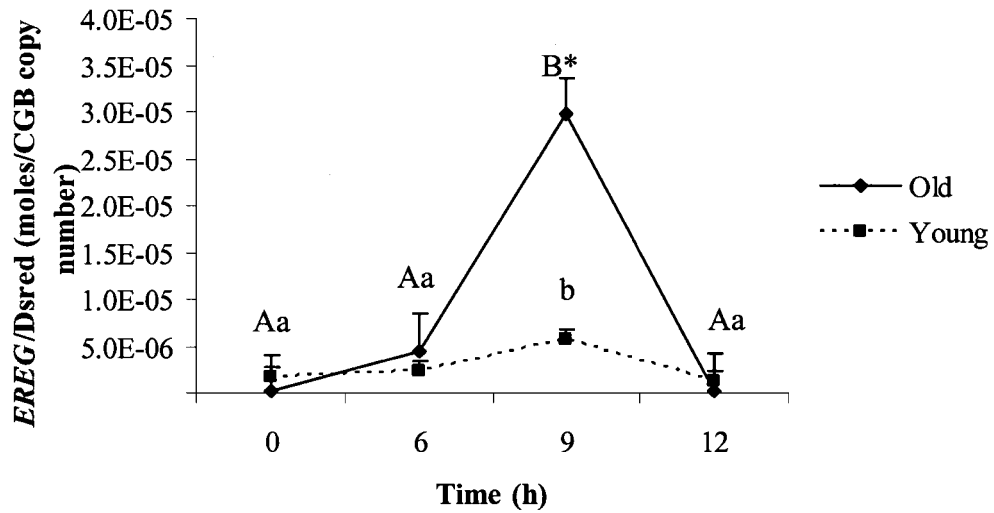


Figure 2. Quantitative expression (means \pm SEM) of *AREG* and *EREG* mRNA in granulosa cells before (0 h) and 6, 9 and 12 h after administration of eLH. ^{AB} Values with different superscripts are different ($P < 0.05$) over time for old mares. ^{ab} Values with different superscript are different ($P < 0.05$) over time for young mares. * $P < 0.05$ young and old mares. Data normalized to DsRed and number of CG β copies.

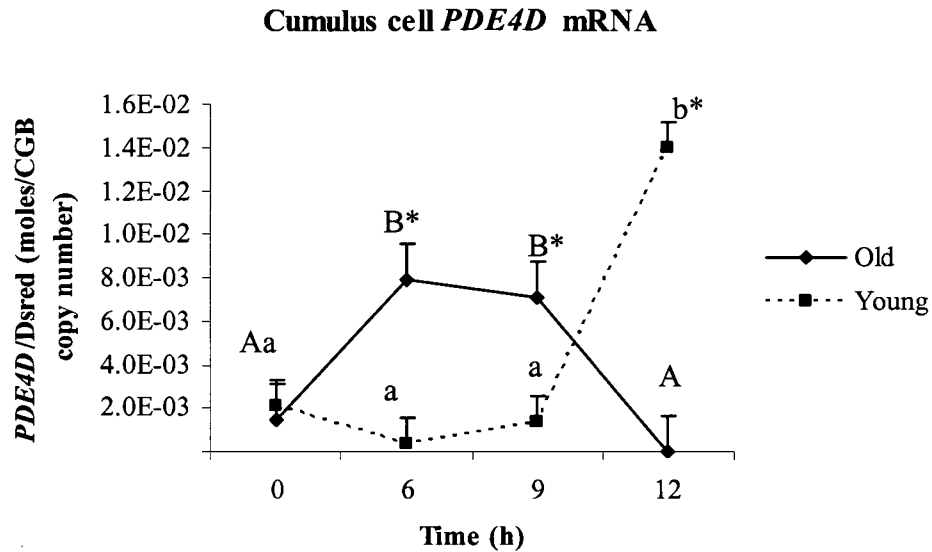
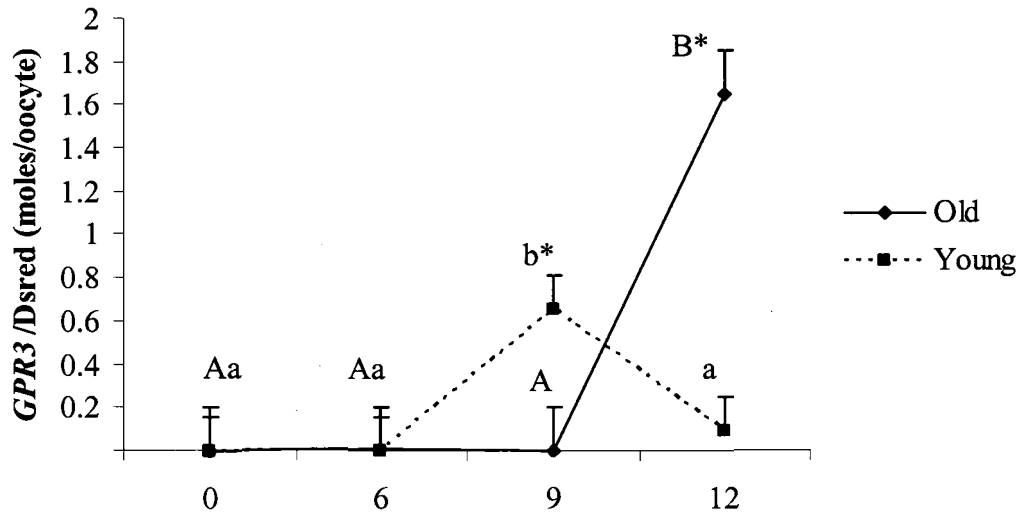


Figure 3. Quantitative expression (means \pm SEM) of *PDE4D* mRNA in cumulus cells before (0 h) and 6, 9 and 12 h after administration of eLH. ^{AB} Values with different superscripts are different ($P < 0.05$) over time for old mares. ^{ab} Values with different superscript are different ($P < 0.05$) over time for young mares. * $P < 0.05$ young and old mares. Data normalized to DsRed and number of CG β copies.

Oocytes

Patterns of expression of *GPR3* mRNA in oocytes of young and old mares were different and elevated ($P < 0.05$) at 9 and 12 h, respectively (Fig. 4). An interaction ($P < 0.05$) in the expression of *GPR3* was observed for age by time at 9 and 12 h. The pattern of expression of *PDE3A* mRNA was similar for oocytes from young and old mares with an increase ($P < 0.05$) at 6 and 9 h. The magnitude of expression for *PDE3A* at 6 and 9 h was higher ($P < 0.05$) for old than young mares (Fig. 4).

Oocyte *GPR3* mRNA



Oocyte *PDE3A* mRNA

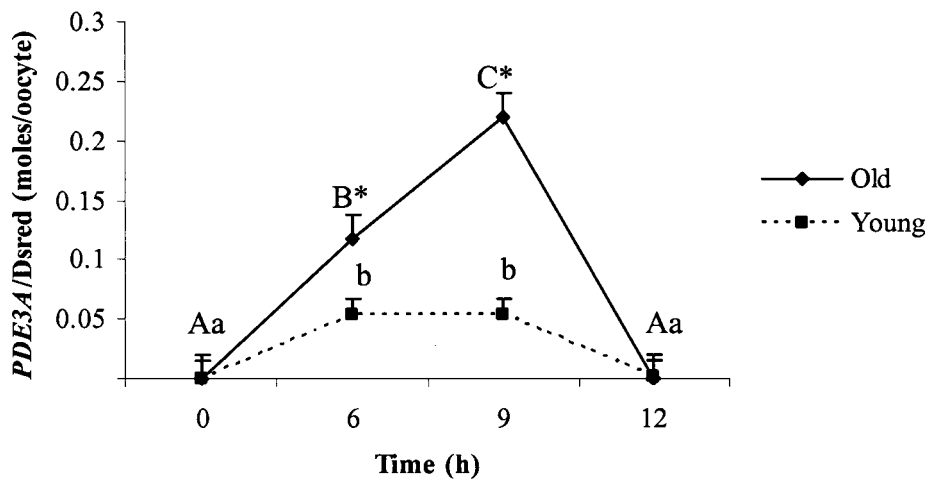
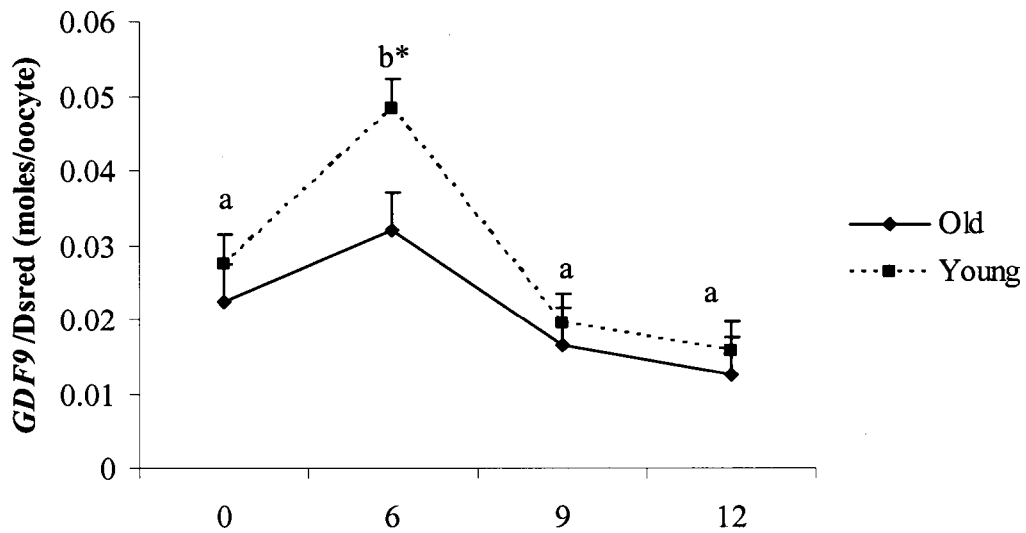


Figure 4. Quantitative expression (means \pm SEM) of *PDE4D* mRNA in cumulus cells before (0 h) and 6, 9 and 12 h after administration of eLH. ^{AB} Values with different superscripts are different ($P < 0.05$) over time for old mares. ^{ab} Values with different superscript are different ($P < 0.05$) over time for young mares. * $P < 0.05$ young and old mares. Data normalized to DsRed and number of CG β copies.

Expression of *GDF9* and *BMP15* mRNA varied for oocytes from young and old mares (Fig. 5). Although both genes appeared to have a similar pattern of expression over time, no significant differences over time were observed for old mares; however, for young mares, expression was higher at 6 h than for the other time points ($P < 0.05$).

Oocyte *GDF9* mRNA



Oocyte *BMP15* mRNA

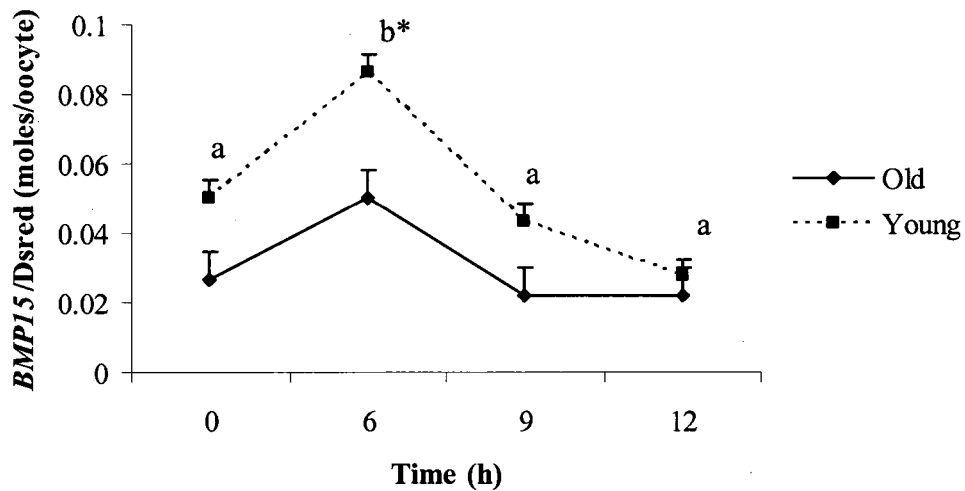


Figure 5. Quantitative expression (means \pm SEM) of *GDF9* and *BMP15* mRNA in oocytes before (0 h) and 6, 9 and 12 h after administration of eLH. ^{ab} Values with different superscript are different ($P < 0.05$) over time for young mares. Values were not different over time for old mares. * $P < 0.05$ young and old mares. Data normalized to DsRed.

Main effects of age were higher ($P < 0.05$) for *GDF9* and *BMP15* in young than old mares. Correlation coefficients between *GDF9* and *BMP15* for old and young mares were 0.94 and 0.99, respectively (Fig. 6).

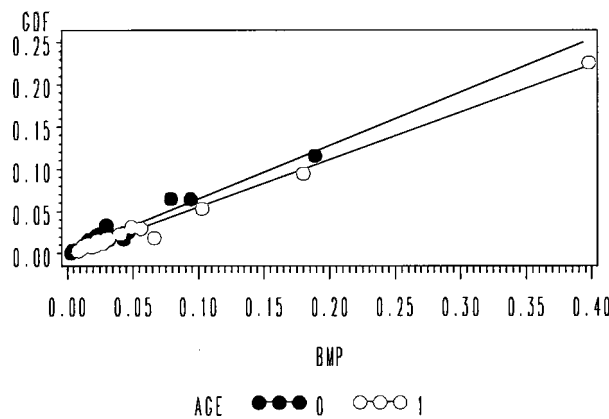


Figure 6. Results from the regression analyses between *GDF9* and *BMP15* for old (0) $R^2=0.94$ and young (1) $R^2=0.99$ mares

The number of copies of oocyte mtDNA did not vary with time after eLH induction of maturation in young mares; however, there was a temporal decrease in oocyte mtDNA copy numbers in old mares (Fig. 7). Corrected mtDNA copy numbers in oocytes tended ($P=0.1$) to be lower in old mares (7×10^5) versus young mares (7.8×10^5).

Oocyte Mitochondrial DNA

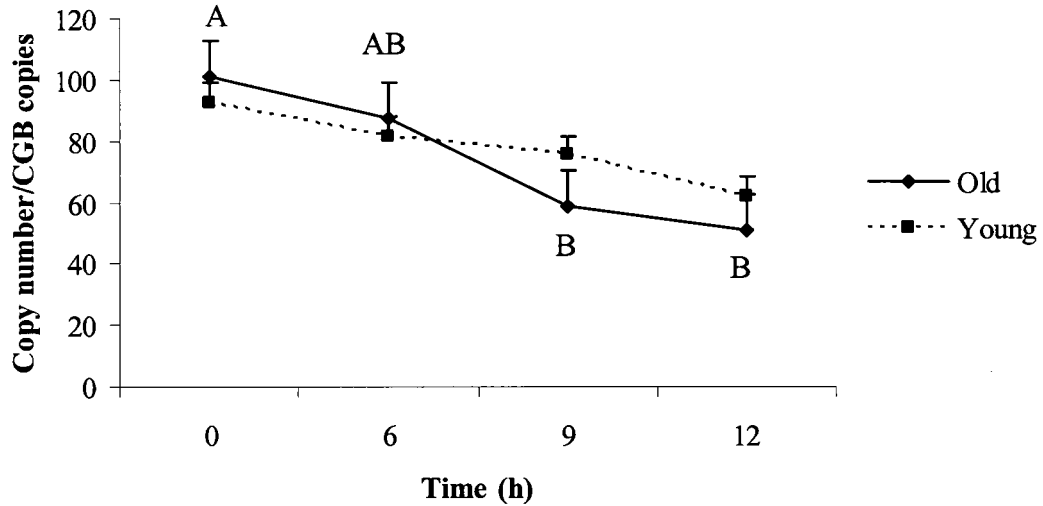


Figure 7. Changes in adjusted copy number (means \pm SEM) of oocyte mitochondrial DNA before (0 h) and 6, 9 and 12 h after administration of eLH. ^{AB} Values with different superscript are different ($P < 0.05$) over time for old mares. Values were not different over time for young mares. Data normalized to mitochondria copies per CG β copies.

Discussion

A number of theories have been proposed to explain the age-associated decline in fertility in women (1,5-8); however, much of the data support the notion that impaired oocyte quality plays a prominent role. The mare could be a valuable nonprimate model to study molecular synchrony of oocyte and follicle maturation as it pertains to the woman, as the species have similarities in follicular dynamics, interval from hCG to ovulation (approximately 36 h) and reproductive aging (12,13,15,16). Thus, in these studies, we used the mare as a model for reproductive ageing and characterized expression of key regulatory genes in the follicular maturation cascade, oocyte-cumulus communications and to quantify oocyte mitochondrial DNA.

The single-chain recombinant eLH used in the present experiment is a chimera constructed with the carboxy terminal end of the eLH β subunit genetically fused to the amino end of the α subunit (132). The half-life of eLH is longer (24 to 48 h) than equine LH (2 to 5 h) in the mare (133). Recombinant eLH is effective at inducing ovulation, without altering endogenous hormone profiles in mares (133).

Follicular maturation is initiated by LH binding to LHRs. The LHRs are confined to mural granulosa cells and external theca cells, although LH ultimately affects cumulus cells and the oocyte (39,48,49). In the horse, numbers of LHRs in the follicle are associated with follicular deviation. Granulosa cells of the dominant follicle have a differential acquisition of *LHR* mRNA just before diameter deviation with evidence of a permissive FSH and estradiol action (44). In the present study, the *LHR* expression profile in granulosa cells was different between young and old mares. Reduced expression of *LHR* was observed in young mares after administration of exogenous eLH; however, no changes in mRNA occurred in the old group, suggesting dysregulation of follicular *LHR* expression. The profile of *LHR* expression in young mares was expected based on studies in other species. In primary cultures of rodent and human granulosa cells, the preovulatory LH surge or exogenous stimulation with hCG or recombinant LH caused a transient and rapid decline in *LHR* expression, uncoupling of the *LHR* from its cognate G protein complex (desensitization), and later an increase in LHR as the corpus luteum developed or cells luteinized in culture (43). Desensitization to LH was described as a Gs uncoupling and loss of hormone stimulated cAMP production, rapid endocytosis of the LHR complex and decreased transcription or degradation of *LHR* mRNA (39,46,47).

Several investigators have shown that, upon LH stimulation, mural granulosa cells function in an autocrine and paracrine fashion to activate a signaling network of EGF-related ligands (AREG and EREG) that induce cumulus expansion, germinal vesicle breakdown and nuclear maturation (48,49,51-54). In the mouse, an ovulatory dose of hCG led to increased expression of *Areg* and *Ereg* mRNAs within 1 to 3 h after injection (48). Furthermore, microarray studies in the mouse indicate maximum levels of *Areg* and *Ereg* are achieved at 2 h after administration of hCG in vivo (51). In our experiment, the expression profile for *AREG* and *EREG* was identical between young and old mares; however, the magnitude of expression was higher in old mares at 6 and 9 h for *AREG* and at 9 h for *EREG*. The findings suggest a higher sensitivity of granulosa cells of older mares to exogenous LH – a finding consistent with higher levels of *LHR* expression in aged mares. Finally, in these studies we do not find any correlation between *AREG* and *EREG* within age groups suggesting that these genes may be independently regulated in the mare..

Phosphodiesterases are essential for oocyte maturation (64-68). Female knock-out *Pde4d* mice had reduced fertility, with a 50% decrease in litter size and decreased cAMP response to gonadotropins, estrogen production, and ovulation rates (60). Expression of *PDE4D* mRNA in cumulus cells increased earlier (6 h) after eLH administration in old mares than in young mares (12 h). This suggests premature upregulation of the *PDE4D* gene in old mares and reduced cAMP for maintenance of oocyte meiotic arrest. If *Pde4d* is a gonadotropin-regulated gene as suggested by Park et al. (62) then this may also reflect an altered time course in LH sensitivity of follicles from aged mares.

The pattern of expression of oocyte-specific *PDE3A* mRNA was similar between young and old mares and equal at 0 and 12 h after injection of eLH. However, the magnitude of expression was higher at 6 and 9 h for old than young mares. In rat oocytes, *Pde3a* is activated before resumption of meiosis in spontaneous and LH-induced maturation in vitro (65). Other oocyte maturation studies have demonstrated a beneficial effect of PDE3A inhibitors on cytoplasmic maturation and blastocyst rate after embryo production in vitro after 16 h of meiotic arrest with PDE3A and 4D inhibitors (72). In humans, exposure of compact oocytes to PDE3A inhibitors during in vitro culture resulted in higher maturation rates and better oocyte morphology; however, fertilization and cleavage rates were the same as controls (73). In the present experiment, the expression profile suggests premature upregulation of *PDE3A* mRNA and, potentially, a premature decrease in oocyte cAMP for old mares and subsequent compromised oocyte developmental competence.

Several investigations have contributed to the understanding of GPR3 function in oocytes of mice and humans. Meiotic arrest in *Gpr3*^{-/-} mouse follicle-enclosed oocytes was rescued by injection of RNA encoding *Gpr3* and its cognate Gs subunit (76,77). Similarly, follicle enclosed mouse oocytes injected with *Gpr3* siRNA, but not with control siRNA, lost their ability to maintain meiotic arrest (78). In humans, *GPR3* mRNA and Gs protein has been detected in immature oocytes. Furthermore, injection of immature human oocytes with Gs antibodies overcame meiotic inhibition of oocytes cultured with cilostamide, a PDE inhibitor (81). In addition, GPR3 is an orphan receptor that acts independently of LH and functions upstream of PDE3A (82,84).

The *GPR3* mRNA expression pattern after induction of maturation was different between young and old mares with peak expression evident at 6 and 12 h post-eLH, respectively. These data further support the notion of age-associated alterations in intra-oocyte levels of cAMP. However, interpretation of this result is difficult, since the ligand of GPR3 is not known. Premature ovarian aging has been documented in mice deficient in *Gpr3*. Decreased fertility was evidenced by reduced numbers of zygotes produced after spontaneous ovulation, increased levels of FSH, shorter estrous cycles, and increased abnormal morphology and fragmentation of oocytes and embryos. Furthermore, development to the two-cell and blastocyst stages was decreased with reductions in implanted embryos and litter size (85). These changes mimic some characteristics associated aging in women (86) and horses (16).

GDF9 and BMP15 belong to the transforming growth factor- β superfamily. Gene expression of GDF9 and BMP15 is primarily confined to oocytes (97). Cellular signaling occurs via a receptor complex involving type I and II of membrane-bound serine/threonine kinases on granulosa cells (91,98). Mouse knock-out models for GDF9 are infertile and show arrested follicular growth at the primary follicle stage. Female *Bmp15* knock-out mice are subfertile, with normal follicular growth but decreased ovulation rates and fertilization failure (99). In cattle, *GDF9* mRNA was abundant in bovine oocytes at 55,000 copies per oocyte and was upregulated in competent oocytes; *BMP15* transcripts were more than 20-fold higher than *GDF9*, and expression of *BMP15* was not associated with oocyte competence (106). Both GDF9 and BMP15 have been used successfully as an additive for bovine in vitro oocyte maturation and embryo production, with blastocyst rates of 51 and 61% per oocyte, respectively, compared to

39% for controls (88). Similarly, supplementation of murine oocytes with GDF9 increased blastocyst cell numbers in the inner cell mass and fetal viability (109). In the present study, the gene expression profiles of *GDF9* and *BMP15* were nearly identical between old and young mares with elevations at 6 h after eLH administration; however, overall expression was higher for both genes in young compared to old mares. The data suggest that lower expression of *GDF9* and *BMP15* in old mares could contribute to poor developmental competence observed clinically in oocytes from old mares (134).

Expression of *GDF9* and *BMP15* were significantly correlated in oocytes of both old and young mares suggesting that there more be convergent gene regulatory pathways for these 2 proteins. GDF9 is expressed in oocytes of primordial follicles in cattle, sheep and hamsters and in primary follicles of humans and rodents whereas BMP15 expression was confined to oocytes of primary follicles (97). Expression of the mature form of BMP15 protein in mice was detected before ovulation but after LH treatment, while GDF9 mature protein was detected before the LH surge (105). Collectively, these data suggest that species differences in timing of *GDF9* and *BMP15* expression are likely.

The mitochondrial genome is maternally transmitted by the oocyte with little or no paternal contribution (116). A genetic bottleneck for the transmission of mtDNA may take place in primordial germ cells (117,125). During oogenesis, mitochondria originate from a small founder population of less than ten mitochondria. These are amplified during oocyte maturation and then reduced. Such restriction and amplification mechanisms seem to reduce the rate of point mutations allowing clonal expansion of a homogeneous set of mtDNA (117). It is thought that one copy of mtDNA exists per mitochondrion (118). In humans, differentiated oogonia carry ~200 copies; ~6000 copies

are present by prophase-I, with 2×10^5 copies of mtDNA by metaphase II (119). In the present experiment, corrected mitochondrial DNA copy numbers in oocytes tended ($p=0.1$) to be lower for old (7.0×10^5) than young (7.8×10^5) mares. Mitochondrial genome copy numbers among and within oocytes of individuals are highly variable. Possibly, the variation is related to the rapid rate of cytoplasmic growth (119) or the pleiomorphic nature of mitochondria, making accurate counting problematic.

Nonetheless, oocyte mitochondrial numbers have been related to developmental competence. In studies using real-time PCR and statistically blocking for male infertility, mtDNA content was lower in cohorts of oocytes from women suffering fertilization failure compared to cohorts with a normal fertilization rate after either in vitro fertilization or intracytoplasmic sperm injection (119,120). In the pig, mtDNA copy number, glucose-6-phosphate dehydrogenase content and cytoplasmic transfer was positively correlated with fertilization outcome (121). In horses, mean numbers of mtDNA copies were reported to be similar between germinal vesicle oocytes from young or aged mares and in vitro matured oocytes from young mares. However, mtDNA copy number of in vitro matured oocytes from aged mares were significantly lower (123). Also, the mitochondria were swollen with extensively damaged cristae.

We find a significant temporal decrease in the number of mitochondrial genome copies in old mares. Constant levels of mtDNA from the MII oocyte to the early embryo have been suggested to reflect a balance between degradation and neosynthesis of mtDNA (125). Potentially, in aged mares, the degradation of oocyte mtDNA is accelerated as compared to young mares, resulting in subfertility at multiple levels during oocyte maturation and subsequent embryo development.

These are the first studies characterizing molecular changes in the follicle and oocyte associated with aging in the horse. Differing expression profiles of *AREG* and *EREG* in granulosa cells, *PDE4D* in cumulus cells, and *PDE3A* and *GPR3* in oocytes support the notion that premature oocyte maturation may be occurring in aged mares. Furthermore, the expression of *LHR* in old mares differs from the profile for young mares suggesting asynchrony of initiation of oocyte and follicle maturation. Total expression levels of *GDF9* and *BMP15* were lower in aged vs. young mare, and aged mare displayed a temporal reduction in mtDNA copy numbers.

CHAPTER IV

GENERAL CONCLUSIONS

The mare is a potential animal model for studying oocyte-follicle physiology and aging in women. Results of this study gave us important insights for the first time in oocyte function and aging in the mare, a monovulatory species. Information in this area is important for our understanding of normal and abnormal equine ovarian function.

We characterized the effects of LH in key regulatory genes involved with the maturation cascade in granulosa and cumulus cells and cumulus-oocyte paracrine communication, as well as quantifying mitochondrial numbers of oocytes obtained from intact follicles before and after recombinant LH treatment. Clinically relevant protocols to improve in vitro equine oocyte maturation may be pertinent to pursue based on the gene expression pattern found in this experiment. Studies including in vitro meiotic arrest with oocyte-specific phosphodiesterase inhibitors and formulations of in vitro maturation media supplemented with GDF9 and BMP15 may be useful. In addition, the LHR potentially can be used as a marker of fertility. The *LHR* mRNA expression in old mares was aberrant when compared to young mares and in-vivo and in-vitro studies done in other species.

Clinical impressions from our assisted reproduction program suggest that oocytes and follicular cells from old mares are morphologically aged when compared to young counterparts following the same treatments. Expression of *AREG*, *EREG* and *PDE3A* mRNA were > 3 fold increased in old mares compared to young mares. In addition, *PDE4D* increased earlier cumulus cells of old mares, suggesting a premature decrease of cAMP and possibly premature aging post LH. Developmental potential of the oocyte is influenced by GDF9, BMP15 and mtDNA. In the present experiment overall gene expression of *GDF9* and *BMP15* from old mares was lower when compared to young mares; also, a linear decrease of mtDNA copy number was found in oocytes from old mares, supporting the idea of poor oocyte competence associated with aging.

More work is necessary in the area of protein expression. The proteins of the candidate genes may not be expressed concomitant with their mRNAs; measuring protein activity would be ideal. However, the number of equine oocytes and follicular cells needed to perform experiments, including western blot analysis and immunocytochemistry can be prohibited by cost.

The key regulator in oocyte maturation is cAMP. Monitoring changes in cAMP of oocytes obtained from each time point and age group could be testable and would corroborate the result of the present experiment. Numbers of oocytes and replications of this experiment may limit the confidence of results. However, single oocyte mRNA quantification provided information without masking individual variability when pools of oocytes are assayed. There is limited information in the literature of monovular animal models with this unique in vivo single cell approach.

CHAPTER V

REFERENCES CITED

1. ESHRE Capri Workshop Group. Fertility and ageing. *Hum Reprod Update* 2005; 11: 261-267
2. Gougeon A. Dynamics of human follicular growth: morphologic, dynamic, and functional aspects. Chapter 2. *The Ovary 2004, Second Edition*. Elsevier Academic Press, Boston
3. Navot D, Bergh PA, Williams MA, Garrisi GJ, Guzman I, Sandler B, Grunfeld L. Poor oocyte quality rather than implantation failure as a cause of age-related decline in female fertility. *Lancet* 1991;337:1375-1377
4. Sauer MV, Paulson RJ, Lobo RA. Reversing the natural decline in human fertility. *J Amer Medical Assoc* 1992;268:1275-1279
5. Ottolenghi C, Uda M, Hamatani T, Crisponi L, Garcia JE, Ko M, Pilia G, Sforza C, Schlessinger D, Forabosco A. Aging of oocyte, ovary, and human reproduction. *Ann N Y Acad Sci*. 2004; 1034:117-131
6. Hsieh RH, Au HK, Wang RS, Yang PS and Tzeng CR. The role of mitochondria in the aging ovary. Chapter 34. *The Ovary 2004, Second Edition*. Elsevier Academic Press, Boston
7. Perez GI, Jurisicova A, Matikainen T, Moriyama T, Kim MR, Takai Y, Pru JK, Kolesnick RN, Tilly JL. A central role for ceramide in the age-related acceleration of apoptosis in the female germline. *FASEB J*. 2005; 19:860-862
8. Gilling-Smith C and Franks S. Ovarian function in assisted reproduction. Chapter 28. *The Ovary 2004, Second Edition*. Elsevier Academic Press, Boston
9. Gilardi KV, Shideler SE, Valverde CR, Roberts JA, Lasley BL. Characterization of the onset of menopause in the rhesus macaque. *Biol Reprod*. 1997; 57:335-40

10. Wu JM, Zelinski MB, Ingram DK, Ottinger MA. Ovarian aging and menopause: current theories, hypotheses, and research models. *Exp Biol Med.* 2005; 230:818-28
11. Malhi PS, Adams GP, Singh J. Bovine model for the study of reproductive aging in women: follicular, luteal, and endocrine characteristics. *Biol Reprod.* 2005; 73:45-53
12. Ginther OJ, Gastal EL, Gastal MO, Bergfelt DR, Baerwald AR, Pierson RA. Comparative study of the dynamics of follicular waves in mares and women. *Biol Reprod.* 2004; 71:1195-1201
13. Ginther OJ, Beg MA, Gastal EL, Gastal MO, Baerwald AR, Pierson RA. Systemic concentrations of hormones during the development of follicular waves in mares and women: a comparative study. *Reproduction.* 2005; 130:379-388
14. Carnevale, E.M., D.R. Bergfelt, O.J. Ginther. Aging effects on follicular activity and concentrations of FSH, LH, and progesterone in mares. *Anim Reprod Sci* 1993; 31:287-299
15. Carnevale, E.M. and O.J. Ginther. Defective oocytes as a cause of subfertility in old mares. *Biol. Reprod. Mono* 1995. 1 (Equine Reproduction VI):209-214
16. Carnevale EM, Griffin PG, Ginther OJ. Age-associated subfertility before entry of the embryo into the uterus in mares. *Equine Vet J*, 1993; 15 (Suppl):31-35
17. Sirard MA, Richard F, Blondin P, Robert C. Contribution of the oocyte to embryo quality. *Theriogenology.* 2006; 65:126-136
18. McLaren A, and Southee D. Entry of mouse embryonic germ cells into meiosis. *Dev Biol.* 1997; 187:107-113
19. Richard FJ. Regulation of meiotic maturation. *J Anim Sci.* 2006; 85(13 Suppl):E4-6.
20. Surani MA. Imprinting and the initiation of gene silencing in the germ line. *Cell.* 1998; 93:309-312
21. Eppig JJ, Viveiros MM, Bivens CM, and de la Fuente R. Regulation of mammalian oocyte maturation. Chapter 7. *The Ovary 2004, Second Edition.* Elsevier Academic Press, Boston
22. Feuerstein P, Cadoret V, Dalbies-Tran R, Guerif F, Royere D. Oocyte-cumulus dialog. *Gynecol Obstet Fertil.* 2006; 34:793-800
23. Eppig JJ, Wigglesworth K, Pendola F, Hirao Y. Murine oocytes suppress expression of luteinizing hormone receptor messenger ribonucleic acid by granulosa cells. *Biol Reprod.* 1997; 56:976-984

24. Assou S, Anahory T, Pantesco V, Le Carrouer T, Pellestor F, Klein B, Reyftmann L, Dechaud H, De Vos J, Hamamah S. The human cumulus-oocyte complex gene-expression profile. *Hum Reprod.* 2006; 21:1705-1719
25. Conti M, Andersen CB, Richard F, Mehats C, Chun SY, Horner K, Jin C, Tsafiri A. Role of cyclic nucleotide signaling in oocyte maturation. *Mol Cell Endocrinol.* 2002; 187:153-159
26. Thomas RE, Thompson JG, Armstrong DT, Gilchrist RB. Effect of specific phosphodiesterase isoenzyme inhibitors during in vitro maturation of bovine oocytes on meiotic and developmental capacity. *Biol Reprod.* 2004; 71:1142-1149
27. Schmidt A, Rauh NR, Nigg EA, Mayer TU. Cytostatic factor: an activity that puts the cell cycle on hold. *J Cell Sci.* 2006; 119:1213-1208.
28. Tunquist BJ, Maller JL. Under arrest: cytotstatic factor (CSF)-mediated metaphase arrest in vertebrate eggs. *Genes Dev.* 2003; 17:683-710
29. Vogt E, Kirsch-Volders M, Parry J, Eichenlaub-Ritter U. Spindle formation, chromosome segregation and the spindle checkpoint in mammalian oocytes and susceptibility to meiotic error. *Mutat Res.* 2008; 651:14-29
30. Andreu-Vieyra C, Lin YN, Matzuk MM. Mining the oocyte transcriptome. *Trends Endocrinol Metab.* 2006; 17:136-143
31. Stitzel ML, Seydoux G. Regulation of the oocyte-to-zygote transition. *Science.* 2007; 316:407-408
32. DeJong J. Basic mechanisms for the control of germ cell gene expression. *Gene.* 2006; 366:39-50
33. Piccioni F, Zappavigna V, Verrotti AC. Translational regulation during oogenesis and early development: the cap-poly(A) tail relationship. *C R Biol.* 2005; 328:863-81
34. Alizadeh Z, Kageyama S, Aoki F. Degradation of maternal mRNA in mouse embryos: selective degradation of specific mRNAs after fertilization. *Mol Reprod Dev.* 2005; 72:281-290
35. Brevini TA, Cillo F, Antonini S, Tosetti V, Gandolfi F. Temporal and spatial control of gene expression in early embryos of farm animals. *Reprod Fertil Dev.* 2007; 19:35-42
36. Fair T, Carter F, Park S, Evans AC, Lonergan P. Global gene expression analysis during bovine oocyte in vitro maturation. *Theriogenology.* 2007 ;68 Suppl 1:91-97

37. Schier AF. The maternal-zygotic transition: death and birth of RNAs. *Science*. 2007; 316:406-407
38. Watanabe T, Totoki Y, Toyoda A, Kaneda M, Kuramochi-Miyagawa S, Obata Y, Chiba H, Kohara Y, Kono T, Nakano T, Surani MA, Sakaki Y, Sasaki H. Endogenous siRNAs from naturally formed dsRNAs regulate transcripts in mouse oocytes. *Nature*. 2008; [Epub ahead of print]
39. Ascoli M, Fanelli F, Segaloff DL. The lutropin/choriogonadotropin receptor, a 2002 perspective. *Endocr Rev*. 2002; 23:141-174
40. Dong C, Filipeanu CM, Duvernay MT, Wu G. Regulation of G protein-coupled receptor export trafficking. *Biochim Biophys Acta*. 2007; 1768:853-870
41. Menon KM, Clouser CL, Nair AK. Gonadotropin receptors: role of post-translational modifications and post-transcriptional regulation. *Endocrine*. 2005; 26:249-257
42. Ziecik AJ, Kaczmarek MM, Blitek A, Kowalczyk AE, Li X, Rahman NA. Novel biological and possible applicable roles of LH/hCG receptor. *Mol Cell Endocrinol*. 2007; 269:51-60
43. Menon KM, Munshi UM, Clouser CL, Nair AK. Regulation of luteinizing hormone/human chorionic gonadotropin receptor expression: a perspective. *Biol Reprod*. 2004; 70:861-866
44. Beg MA, Ginther OJ. Follicle selection in cattle and horses: role of intrafollicular factors. *Reproduction*. 2006 ;132:365-377
45. Beg MA, Bergfelt DR, Kot K, Wiltbank MC, Ginther OJ. Follicular-fluid factors and granulosa-cell gene expression associated with follicle deviation in cattle. *Biol Reprod*. 2001; 64:432-441
46. Menon KM, Nair AK, Wang L, Peegel H. Regulation of luteinizing hormone receptor mRNA expression by a specific RNA binding protein in the ovary. *Mol Cell Endocrinol*. 2007; 260-262:109-116
47. Nair AK, Peegel H, Menon KM. The role of luteinizing hormone/human chorionic gonadotropin receptor-specific mRNA binding protein in regulating receptor expression in human ovarian granulosa cells. *J Clin Endocrinol Metab*. 2006; 91:2239-2243
48. Park JY, Su YQ, Ariga M, Law E, Jin SL, Conti M. EGF-like growth factors as mediators of LH action in the ovulatory follicle. *Science*. 2004; 303:682-684

49. Hsieh M, Lee D, Panigone S, Horner K, Chen R, Theologis A, Lee DC, Threadgill DW, Conti M. Luteinizing hormone-dependent activation of the epidermal growth factor network is essential for ovulation. *Mol Cell Biol.* 2007; 27:1914-1924
50. Prenzel N, Zwick E, Daub H, Leserer M, Abraham R, Wallasch C, Ullrich A. EGF receptor transactivation by G-protein-coupled receptors requires metalloproteinase cleavage of proHB-EGF. *Nature.* 1999; 402:884-888
51. Conti M, Hsieh M, Park JY, Su YQ. Role of the epidermal growth factor network in ovarian follicles. *Mol Endocrinol.* 2006; 20:715-723
52. Panigone S, Hsieh M, Fu M, Persani L, Conti M. LH Signaling in Preovulatory Follicles Involves Early Activation of the EGFR Pathway. *Mol Endocrinol.* 2008 Jan 10; [Epub ahead of print]
53. Shimada M, Hernandez-Gonzalez I, Gonzalez-Robayna I, Richards JS. Paracrine and autocrine regulation of epidermal growth factor-like factors in cumulus oocyte complexes and granulosa cells: key roles for prostaglandin synthase 2 and progesterone receptor. *Mol Endocrinol.* 2006; 20:1352-1365
54. Ashkenazi H, Cao X, Motola S, Popliker M, Conti M, Tsafirri A. Epidermal growth factor family members: endogenous mediators of the ovulatory response. *Endocrinology.* 2005; 146:77-84
55. Campos-Chillon LF, Clay CM, Altermatt JL, Bouma GL and Carnevale EM. Differences in resumption of oocyte maturation in young and old mares. *Reprod Fertil Dev.* 2008; 20:81
56. Shimada M, Hernandez-Gonzalez I, Gonzalez-Robayna I, Richards JS. Induced expression of pattern recognition receptors in cumulus oocyte complexes: novel evidence for innate immune-like functions during ovulation. *Mol Endocrinol.* 2006; 20:3228-3239
57. Conti M, Nemoz G, Sette C, Vicini E. Recent progress in understanding the hormonal regulation of phosphodiesterases. *Endocr Rev.* 1995; 16:370-389
58. Vicini E, Conti M. Characterization of an intronic promoter of a cyclic adenosine 3',5'-monophosphate (cAMP)-specific phosphodiesterase gene that confers hormone and cAMP inducibility. *Mol Endocrinol.* 1997; 11:839-850
59. Swinnen JV, Joseph DR, Conti M. The mRNA encoding a high-affinity cAMP phosphodiesterase is regulated by hormones and cAMP. *Proc Natl Acad Sci USA.* 1989; 86:8197-8201

60. Jin SL, Richard FJ, Kuo WP, D'Ercole AJ, Conti M. Impaired growth and fertility of cAMP-specific phosphodiesterase PDE4D-deficient mice. *Proc Natl Acad Sci USA*. 1999; 96:11998-12003
61. Tsafiriri A, Chun SY, Zhang R, Hsueh AJ, Conti M. Oocyte maturation involves compartmentalization and opposing changes of cAMP levels in follicular somatic and germ cells: studies using selective phosphodiesterase inhibitors. *Dev Biol*. 1996; 178:393-402
62. Park JY, Richard F, Chun SY, Park JH, Law E, Horner K, Jin SL, Conti M. Phosphodiesterase regulation is critical for the differentiation and pattern of gene expression in granulosa cells of the ovarian follicle. *Mol Endocrinol*. 2003; 17:1117-1130
63. Thomas RE, Armstrong DT, Gilchrist RB. Differential effects of specific phosphodiesterase isoenzyme inhibitors on bovine oocyte meiotic maturation. *Dev Biol*. 2002; 244:215-225
64. Mayes MA, Sirard MA. Effect of type 3 and type 4 phosphodiesterase inhibitors on the maintenance of bovine oocytes in meiotic arrest. *Biol Reprod*. 2002; 66:180-184
65. Richard FJ, Tsafiriri A, Conti M. Role of phosphodiesterase type 3A in rat oocyte maturation. *Biol Reprod*. 2001; 65:1444-1451
66. Conti M, Andersen CB, Richard F, Mehats C, Chun SY, Horner K, Jin C, Tsafiriri A. Role of cyclic nucleotide signaling in oocyte maturation. *Mol Cell Endocrinol*. 2002; 187:153-159
67. Han SJ, Vaccari S, Nedachi T, Andersen CB, Kovacina KS, Roth RA, Conti M. Protein kinase B/Akt phosphorylation of PDE3A and its role in mammalian oocyte maturation. *EMBO J*. 2006; 25:5716-5725
68. Masciarelli S, Horner K, Liu C, Park SH, Hinckley M, Hockman S, Nedachi T, Jin C, Conti M, Manganiello V. Cyclic nucleotide phosphodiesterase 3A-deficient mice as a model of female infertility. *J Clin Invest*. 2004; 114:196-205
69. Sasseville M, Côté N, Guillemette C, Richard FJ. New insight into the role of phosphodiesterase 3A in porcine oocyte maturation. *BMC Dev Biol*. 2006; 6:47
70. Bornslaeger EA, Mattei P, Schultz RM. Involvement of cAMP-dependent protein kinase and protein phosphorylation in regulation of mouse oocyte maturation. *Dev Biol*. 1986; 114:453-462
71. Nogueira D, Cortvrindt R, Everaerd B, Smits J. Effects of long-term in vitro exposure to phosphodiesterase type-3 inhibitors on follicle and oocyte development. *Reproduction*. 2005; 130:177-186

72. Thomas RE, Thompson JG, Armstrong DT, Gilchrist RB. Effect of specific phosphodiesterase isoenzyme inhibitors during in vitro maturation of bovine oocytes on meiotic and developmental capacity. *Biol Reprod.* 2004; 71:1142-1149
73. Nogueira D, Ron-El R, Friedler S, Schachter M, Raziel A, Cortvrindt R, Smitz J. Meiotic arrest in vitro by phosphodiesterase 3-inhibitor enhances maturation capacity of human oocytes and allows subsequent embryonic development. *Biol Reprod.* 2006; 74:177-184
74. Eggerickx D, Deneff JF, Labbe O, Hayashi Y, Refetoff S, Vassart G, Parmentier M, Libert F. Molecular cloning of an orphan G-protein-coupled receptor that constitutively activates adenylate cyclase. *Biochem J.* 1995; 309:837-843
75. Uhlenbrock K, Gassenhuber H, Kostenis E. Sphingosine 1-phosphate is a ligand of the human gpr3, gpr6 and gpr12 family of constitutively active G protein-coupled receptors. *Cell Signal.* 2002; 14:941-953
76. Mehlmann LM, Saeki Y, Tanaka S, Brennan TJ, Evsikov AV, Pendola FL, Knowles BB, Eppig JJ, Jaffe LA. The Gs-linked receptor GPR3 maintains meiotic arrest in mammalian oocytes. *Science.* 2004; 306:1947-1950
77. Mehlmann LM. Stops and starts in mammalian oocytes: recent advances in understanding the regulation of meiotic arrest and oocyte maturation. *Reproduction.* 2005; 130:791-799
78. Mehlmann LM. Oocyte-specific expression of Gpr3 is required for the maintenance of meiotic arrest in mouse oocytes. *Dev Biol.* 2005; 288:397-404
79. Hinckley M, Vaccari S, Horner K, Chen R, Conti M. The G-protein-coupled receptors GPR3 and GPR12 are involved in cAMP signaling and maintenance of meiotic arrest in rodent oocytes. *Dev Biol.* 2005; 287:249-261
80. Freudzon L, Norris RP, Hand AR, Tanaka S, Saeki Y, Jones TL, Rasenick MM, Berlot CH, Mehlmann LM, Jaffe LA. Regulation of meiotic prophase arrest in mouse oocytes by GPR3, a constitutive activator of the Gs G protein. *J Cell Biol.* 2005; 171:255-265
81. Diluigi A, Weitzman VN, Pace MC, Siano LJ, Maier D, Mehlmann LM. Meiotic arrest in human oocytes is maintained by a gs signaling pathway. *Biol Reprod.* 2008; 78:667-672
82. Norris RP, Freudzon L, Freudzon M, Hand AR, Mehlmann LM, Jaffe LA. A G(s)-linked receptor maintains meiotic arrest in mouse oocytes, but luteinizing hormone

- does not cause meiotic resumption by terminating receptor-G(s) signaling. *Dev Biol.* 2007; 310:240-249
83. Mehlmann LM, Kalinowski RR, Ross LF, Parlow AF, Hewlett EL, Jaffe LA. Meiotic resumption in response to luteinizing hormone is independent of a Gi family G protein or calcium in the mouse oocyte. *Dev Biol.* 2006 15; 299:345-355
84. Vaccari S, Horner K, Mehlmann LM, Conti M. Generation of mouse oocytes defective in cAMP synthesis and degradation: Endogenous cyclic AMP is essential for meiotic arrest. *Dev Biol.* 2008; 316:124-134
85. Ledent C, Demeestere I, Blum D, Petermans J, Hamalainen T, Smits G, Vassart G. Premature ovarian aging in mice deficient for Gpr3. *Proc Natl Acad Sci U S A.* 2005; 102:8922-8926
86. te Velde ER, Pearson PL. The variability of female reproductive ageing. *Hum Reprod Update.* 2002; 8:141-154
87. Kovanci E, Simpson JL, Amato P, Rohozinski J, Heard MJ, Bishop CE, Carson SA. Oocyte-specific G-protein-coupled receptor 3 (GPR3): no perturbations found in 82 women with premature ovarian failure (first report). *Fertil Steril.* 2007 Oct; [Epub ahead of print]
88. Hussein TS, Thompson JG, Gilchrist RB. Oocyte-secreted factors enhance oocyte developmental competence. *Dev Biol.* 2006; 296:514-521
89. Pangas SA, Matzuk MM. The art and artifact of GDF9 activity: cumulus expansion and the cumulus expansion-enabling factor. *Biol Reprod.* 2005; 73:582-585
90. Matzuk MM, Burns KH, Viveiros MM, Eppig JJ. Intercellular communication in the mammalian ovary: oocytes carry the conversation. *Science.* 2002; 296:2178-2180
91. Juengel JL, Bodensteiner KJ, Heath DA, Hudson NL, Moeller CL, Smith P, Galloway SM, Davis GH, Sawyer HR, McNatty KP. Physiology of GDF9 and BMP15 signaling molecules. *Anim Reprod Sci.* 2004; 82-83:447-460
92. Carabatsos MJ, Sellitto C, Goodenough DA, Albertini DF. Oocyte-granulosa cell heterologous gap junctions are required for the coordination of nuclear and cytoplasmic meiotic competence. *Dev Biol.* 2000; 226:167-179
93. Ackert CL, Gittens JE, O'Brien MJ, Eppig JJ, Kidder GM. Intercellular communication via connexin 43 gap junctions is required for ovarian folliculogenesis in the mouse. *Dev Biol.* 2001; 233:258-270

94. Kidder GM, Mhawi AA. Gap junctions and ovarian folliculogenesis. *Reproduction*. 2002;123:613-620
95. Sela-Abramovich S, Edry I, Galiani D, Nevo N, Dekel N. Disruption of gap junctional communication within the ovarian follicle induces oocyte maturation. *Endocrinology*. 2006;147:2280-2286
96. Edry I, Sela-Abramovich S, Dekel N. Meiotic arrest of oocytes depends on cell-to-cell communication in the ovarian follicle. *Mol Cell Endocrinol*. 2006; 252:102-106
97. Juengel JL, McNatty KP. The role of proteins of the transforming growth factor-beta superfamily in the intraovarian regulation of follicular development. *Hum Reprod Update*. 2005; 11:143-160
98. Dragovic RA, Ritter LJ, Schulz SJ, Amato F, Thompson JG, Armstrong DT, Gilchrist RB. Oocyte-secreted factor activation of SMAD 2/3 signaling enables initiation of mouse cumulus cell expansion. *Biol Reprod*. 2007; 76:848-857
99. Yan C, Wang P, DeMayo J, DeMayo FJ, Elvin JA, Carino C, Prasad SV, Skinner SS, Dunbar BS, Dube JL, Celeste AJ, Matzuk MM. Synergistic roles of bone morphogenetic protein 15 and growth differentiation factor 9 in ovarian function. *Mol Endocrinol*. 2001; 15:854-866
100. Yoshino O, McMahon HE, Sharma S, Shimasaki S. unique preovulatory expression pattern plays a key role in the physiological functions of BMP-15 in the mouse. *Proc Natl Acad Sci U S A*. 2006; 103:10678-10683
101. Sugiura K, Su YQ, Diaz FJ, Pangas SA, Sharma S, Wigglesworth K, O'Brien MJ, Matzuk MM, Shimasaki S, Eppig JJ. Oocyte-derived BMP15 and FGFs cooperate to promote glycolysis in cumulus cells. *Development*. 2007; 134:2593-2603
102. Su YQ, Sugiura K, Wigglesworth K, O'Brien MJ, Affourtit JP, Pangas SA, Matzuk MM, Eppig JJ. Oocyte regulation of metabolic cooperativity between mouse cumulus cells and oocytes: BMP15 and GDF9 control cholesterol biosynthesis in cumulus cells. *Development*. 2008; 135:111-121
103. Spicer LJ, Aad PY, Allen DT, Mazerbourg S, Payne AH, Hsueh AJ. Growth differentiation factor 9 (GDF9) stimulates proliferation and inhibits steroidogenesis by bovine theca cells: influence of follicle size on responses to GDF9. *Biol Reprod*. 2008; 78:243-253
104. Hussein TS, Froiland DA, Amato F, Thompson JG, Gilchrist RB. Oocytes prevent cumulus cell apoptosis by maintaining a morphogenic paracrine gradient of bone morphogenetic proteins. *J Cell Sci*. 2005; 118:5257-5268

105. Gilchrist RB, Lane M, Thompson JG. Oocyte-secreted factors: regulators of cumulus cell function and oocyte quality. *Hum Reprod Update*. 2008; 14:159-177
106. Donnison M, Pfeffer PL. Isolation of genes associated with developmentally competent bovine oocytes and quantitation of their levels during development. *Biol Reprod*. 2004; 71:1813-1821
107. Chand AL, Ponnampalam AP, Harris SE, Winship IM, Shelling AN. Mutational analysis of BMP15 and GDF9 as candidate genes for premature ovarian failure. *Fertil Steril*. 2006; 86:1009-1012
108. Thomas FH, Vanderhyden BC. Oocyte-granulosa cell interactions during mouse follicular development: regulation of kit ligand expression and its role in oocyte growth. *Reprod Biol Endocrinol*. 2006; 4:19
109. Yeo CX, Gilchrist RB, Thompson JG, Lane M. Exogenous growth differentiation factor 9 in oocyte maturation media enhances subsequent embryo development and fetal viability in mice. *Hum Reprod*. 2008; 23:67-73
110. Jansen RP, Burton GJ. Mitochondrial dysfunction in reproduction. *Mitochondrion*. 2004; (5-6):577-600
111. Dumollard R, Ward Z, Carroll J, Duchen MR. Regulation of redox metabolism in the mouse oocyte and embryo. *Development*. 2007;134:455-465
112. Shoubridge EA, Wai T. Mitochondrial DNA and the mammalian oocyte. *Curr Top Dev Biol*. 2007;77:87-111
113. Perez GI, Trbovich AM, Gosden RG, Tilly JL. Mitochondria and the death of oocytes. *Nature*. 2000; 403:500-501
114. Van Blerkom J. Mitochondria in human oogenesis and preimplantation embryogenesis: engines of metabolism, ionic regulation and developmental competence. *Reproduction*. 2004 ;128:269-280
115. Larsen NB, Rasmussen M, Rasmussen LJ. Nuclear and mitochondrial DNA repair: similar pathways? *Mitochondrion*. 2005; 5:89-108
116. Sutovsky P, Moreno RD, Ramalho-Santos J, Dominko T, Simerly C, Schatten G. Ubiquitinated sperm mitochondria, selective proteolysis, and the regulation of mitochondrial inheritance in mammalian embryos. *Biol Reprod*. 2000; 63:582-590
117. Jansen RP, de Boer K. The bottleneck: mitochondrial imperatives in oogenesis and ovarian follicular fate. *Mol Cell Endocrinol*. 1998; 145:81-88

118. Thundathil J, Filion F, Smith LC. Molecular control of mitochondrial function in preimplantation mouse embryos. *Mol Reprod Dev.* 2005; 71:405-413
119. Reynier P, May-Panloup P, Chrétien MF, Morgan CJ, Jean M, Savagner F, Barrière P, Malthiery Y. Mitochondrial DNA content affects the fertilizability of human oocytes. *Mol Hum Reprod.* 2001; 7:425-429
120. Santos TA, El Shourbagy S, St John JC. Mitochondrial content reflects oocyte variability and fertilization outcome. *Fertil Steril.* 2006; 85:584-591
121. El Shourbagy SH, Spikings EC, Freitas M, St John JC. Mitochondria directly influence fertilisation outcome in the pig. *Reproduction.* 2006;131:233-245
122. Rambags BP, van Boxtel DC, Tharasanit T, Lenstra JA Colenbrander B, Stout TA. Maturation in vitro leads to mitochondrial degeneration in oocytes recovered from aged but not young mares. *Animal Reproduction Science.* 2006; 94:359-361
123. Torner H, Alm H, Kanitz W, Goellnitz K, Becker F, Poehland R, Bruessow KP, Tuchscherer A. Effect of initial cumulus morphology on meiotic dynamic and status of mitochondria in horse oocytes during IVM. *Reprod Domest Anim.* 2007; 42:176-183
124. Takeuchi T, Neri QV, Katagiri Y, Rosenwaks Z, Palermo GD. Effect of treating induced mitochondrial damage on embryonic development and epigenesis. *Biol Reprod.* 2005; 72:584-592
125. McConnell JM, Petrie L. Mitochondrial DNA turnover occurs during preimplantation development and can be modulated by environmental factors. *Reprod Biomed Online.* 2004; 9:418-424
126. Kujoth GC, Hiona A, Pugh TD, Someya S, Panzer K, Wohlgemuth SE, Hofer T, Seo AY, Sullivan R, Jobling WA, Morrow JD, Van Remmen H, Sedivy JM, Yamasoba T, Tanokura M, Weindruch R, Leeuwenburgh C, Prolla TA. Mitochondrial DNA mutations, oxidative stress, and apoptosis in mammalian aging. *Science.* 2005; 309:481-484
127. Chan CC, Liu VW, Lau EY, Yeung WS, Ng EH, Ho PC. Mitochondrial DNA content and 4977 bp deletion in unfertilized oocytes. *Mol Hum Reprod.* 2005; 11:843-846
128. Lechniak D. Quantitative aspect of gene expression analysis in mammalian oocytes and embryos. *Reprod Biol.* 2002; 2:229-241

129. Vigneault C, Gilbert I, Sirard MA, Robert C. Using the histone H2a transcript as an endogenous standard to study relative transcript abundance during bovine early development. *Mol Reprod Dev.* 2007; 74:703-715
130. Coutinho da Silva MA, Carnevale EM, Maclellan LJ, Seidel GE Jr, Squires EL. Effect of time of oocyte collection and site of insemination on oocyte transfer in mares. *J Anim Sci* 2002; 80:1275-1279.
131. Lindbloom M, Farmerie TA, Clay CM, Seidel GE, Carnevale EM. Potential involvement of EGF-like growth factors and phosphodiesterases in initiation of equine oocyte maturation. *Anim Reprod Sci* 2008; 103(1-2):187-92.
132. Jablonka-Shariff A, Roser JF, Bousfield GR, Wolfe MW, Sibley LE, Colgin M, Boime I. Expression and bioactivity of a single chain recombinant equine luteinizing hormone (reLH). *Theriogenology* 2007; 67:311-320.
133. Yoon MJ, Boime I, Colgin M, Niswender KD, King SS, Alvarenga M, Jablonka-Shariff A, Pearl CA, Roser JF. The efficacy of a single chain recombinant equine luteinizing hormone (reLH) in mares: Induction of ovulation, hormone profiles, and inter-ovulatory intervals. *Dom Anim Endocrinol* 2007; 33:470-479.
134. Carnevale EM. The mare model for follicular maturation and reproductive aging in the woman. *Theriogenology* 2008; 69:23-30.

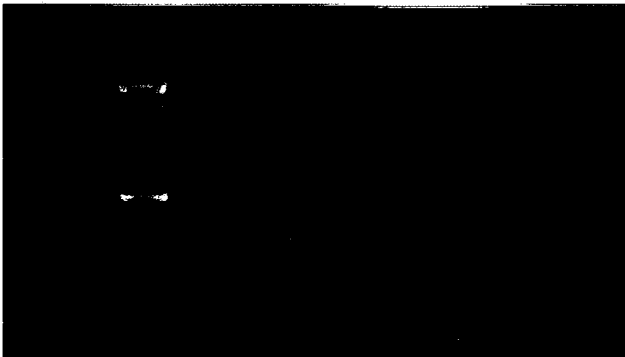
CHAPTER VI

APPENDIX

Gene cell type specificity

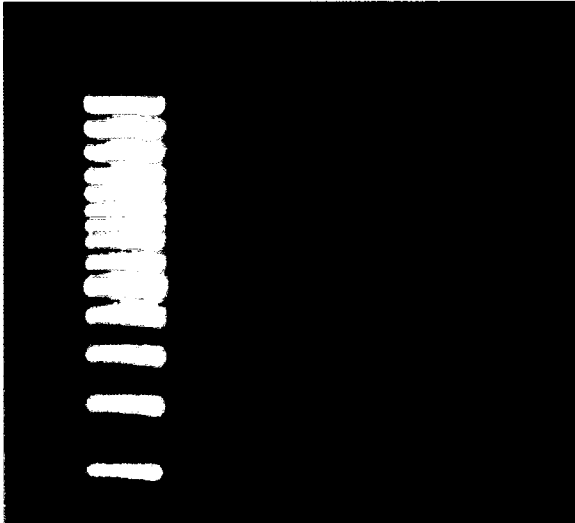
1. LHR PCR of cDNA of oocyte (A), genomic DNA (B), cDNA of cumulus (C) and granulosa (D) cells. Product size 271 bp

Lader A B C D



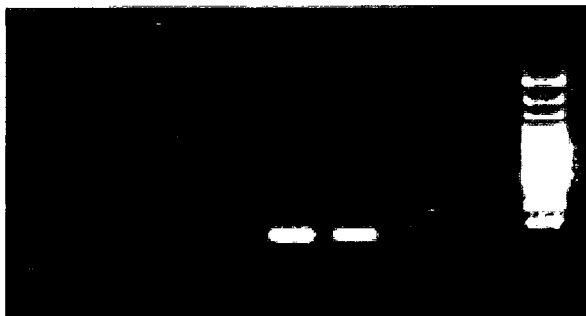
2. AREG PCR of genomic DNA (A), cDNA of oocyte (B) , cumulus (C) and granulosa (D) cells. Product size 132 bp

Lader A B C D



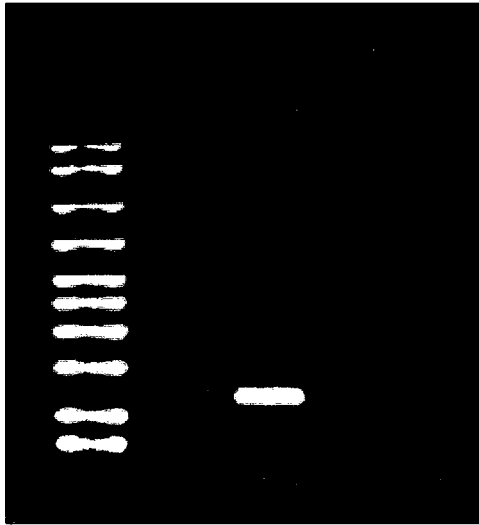
3. EREG PCR of genomic DNA (A), cDNA of granulosa (B) , cumulus (C) cells and cDNA of oocyte (D). Product size 53 bp

A B C D Lader



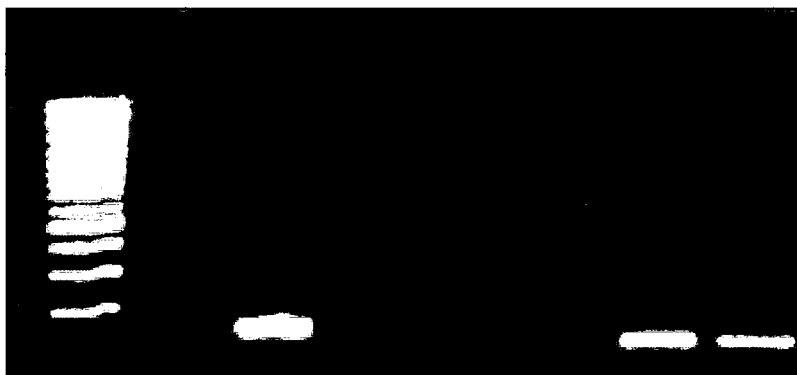
4. PDE4D PCR of cDNA of cumulus cells (A), genomic DNA (B), and cDNA of oocyte (C). Product size 269 bp

Ladder A B C



5. GPR3 PCR of cDNA of granulosa cells (A), genomic DNA (B), cDNA of cumulus (C) and oocyte (D). Product size 154 bp

Ladder A B C B D



6. PDE3A PCR of cDNA of oocyte (A), cDNA of granulosa (B), cumulus (C) cells and genomic DNA (D). Product size 173 bp

Ladder A B C D



7. GDF9 PCR of cDNA of oocyte (A), genomic DNA (B), cDNA of granulosa (C) and cumulus (D) cells. Product size 150 bp

Ladder A B A C D



8. BMP15 PCR of cDNA of oocyte (A), cDNA of granulosa (B), cumulus (C) cells and genomic DNA(D). Product size 175 bp

Ladder A B C A D

